Hindawi
Journal of Electrical and Computer Engineering
Volume 2022, Article ID 4044757, 25 pages
https://doi.org/10.1155/2022/4044757

Research Article

Wind Energy Resource Prediction and Optimal Storage Sizing to Guarantee Dispatchability: A Case Study in the Kenyan Power Grid

Hampfrey Odero,[1] **Cyrus Wekesa**,[2] **and George Irungu**[3]

[1]*Department of Electrical Engineering, Pan African University, Institute for Basic Sciences, Technology and Innovation, Nairobi 62000-00200, Kenya*
[2]*School of Engineering, University of Eldoret, Eldoret 1125-30100, Kenya*
[3]*Department of Electrical and Electronic Engineering, Jomo Kenyatta University of Agriculture and Technology, Nairobi 62000-00200, Kenya*

Correspondence should be addressed to Hampfrey Odero; odero.hampfrey@students.jkuat.ac.ke

Received 17 March 2022; Accepted 26 April 2022; Published 28 May 2022

Academic Editor: François Vallée

Kenya is experiencing a fast increase in grid-connected intermittent renewable energy sources (RESs) to meet its increased power demand, and at the same time be able to fulfill its Paris Agreement obligations of abating greenhouse gas emissions. For instance, Kenya has 102 MW of grid-tied solar power and 410 MW of grid-tied wind power. However, these sources are very intermittent with low predictability. Thus, after their installation and integration into the grid, they impose a new challenge for the secure, reliable, and economic operation of the system. To mitigate these and to ensure proper planning of the system operations, accurate and faster prediction of the generation output of the wind energy resources and optimal design and sizing of storage for the large-scale wind energy integration into the grid are of paramount importance. Artificial intelligence (AI) and metaheuristic techniques have proven to be efficient and robust in offering solutions to complex nonlinear prediction and optimization problems. Therefore, this study aims to utilize backpropagation neural network (BPNN) algorithm to conduct hourly prediction of the generation output of Lake Turkana Wind Power Plant (LTWPP), a 310 MW plant connected to the Kenyan power grid, and optimally size its battery energy storage system (BESS) using genetic algorithm (GA) to guarantee its dispatchability. The historical weather data, namely wind speed, ambient temperature, relative humidity, wind direction, and generation output from LTWPP, are employed in the training, testing, and validation of the neural network. LTWPP and BESS are modelled in MATLAB R2016a software. Thereafter, the developed BPNN and GA algorithms are applied to the modelled systems to predict the wind output and optimize the storage system, respectively. BESS optimization with neural prediction reduces the BESS capacity and investment costs by 59.82%, while the overall dispatchability of LTWPP is increased from 73.36% to 90.14%, hence enabling the farm to meet its allowable loss of power supply probability (LPSP) index of 0.1 while guaranteeing its dispatchability.

1. Introduction

The utilization of renewable energy sources (RESs) has experienced remarkable growth in electrical grids worldwide. This is attributed largely to critical factors, namely a fast and unprecedented surge in volatile fuel prices, the scarcity of available primary energy resources utilized in conventional power plants, and the need to abate greenhouse gas emissions.

Wind power constitutes the renewable energy technology (RET) that has exhibited swift growth in comparison to other RETs being investigated currently. The capacity of wind worldwide is far larger than the world's total energy consumption and the potential for development is substantial [1]. Globally, total capacities of about 651 GW of wind have been installed, with a yearly production of 60.4 GW in 2019 alone [2]. By 2023, it is foreseen that RES will be able to supply above 70% of the increase in electricity generation worldwide, with wind and solar taking the lead positions [3].

In Kenya, for example, at the beginning of the last decade, wind energy constituted only 0.24% of the total share

of electricity generation. This has grown tremendously to constitute 11.74% by the end of the same decade, with still many more planned or incepted wind energy projects such as 100 MW Aeolus Ngong' Wind and 60 MW Aperture Green Ngong', among many others mentioned in [1]. The least-cost generation simulation included wind as a candidate project in Kenya for system optimization [4]. Still, there is a small level of competency and expertise in utilizing wind energy for large-scale power production in Kenya. Nevertheless, interest and awareness are gradually growing. The latest large investment in wind power is the 310 MW Lake Turkana Wind farm, the largest in Africa. LTWPP was anticipated not only to reduce the overall cost of energy but to reduce the greenhouse gas emission, hence placing it as a competitive energy source.

However, these merits and development of wind power come with several challenges while integrating it with the existing grids. These include erratic wind flow patterns/profiles which might introduce harmonics into the grid, interfere with the voltage levels, affect grid stability, and bring about unit commitment and scheduling problems [5–7]. To take care of these shortcomings, AI techniques such as artificial neural network (ANN) play a critical role in the development of faster and cheaper predictions for short-term, intermediate, and long-term predictions.

Recently, several wind impact researches have been conducted in various parts of the world in an attempt to address those challenges. The outcomes of these researches are normally linked to different aspects of wind power, notably its randomly varying nature, generator technologies, and sizing of the storage of the wind energy resources (WERs). Very few studies of that nature have been carried out in Kenya despite the increasing WER development projects. In January 2021, Clir Renewables, a Canadian software company, signed a contract with LTWPP to optimize power generation at the power station with the overall objective of improving the efficiency of the power plant, improving power output (reducing unnecessary turbine downtime), and grid stability [8].

In addition, it is worth noting that very few studies have integrated both the wind energy prediction and optimal storage sizing. In [9], the simulation performed demonstrated the efficiency of predicting the RES using a high-order neural network trained with an extended Kalman filter (EKF) and optimally sizing the grid-connected storage system utilizing both the GA and clonal selection algorithms to reduce CO_2 emissions. Thus, there is a need to conduct studies to efficiently and precisely analyze and predict the fluctuating weather patterns associated with such renewables and be able to perform optimal storage designs that will make the grid robust and reliable in its operations. This study has explored a different prediction algorithm, that is, BPNN trained with Levenberg–Marquardt (LM) optimization and optimally sizing its BESS using GA to guarantee the dispatchability of LTWPP.

Despite the fact that Kenya has the largest wind power plant in Africa and is experiencing a fast growth of intermittent renewable sources, it does not have any BESS installations. This study therefore attempts to solve an existing problem that at the moment there is no available documentation that shows there is previous research that has been done on the same. The problem is that of the intermittent power output of WER at LTWPP which requires to be minimized so that the plant output can be dispatchable just like the other plants (geothermal, heavy fuel oil, and hydros) connected in the same grid. This intermittency has caused serious problems to the spinning generators having to undergo excessive hunting. This hunting has led to extensive bearing damages to the other generators called upon to either increase or decrease their outputs during intermittency periods. By researching the LTWPP output characteristic and arriving at the approximate contribution of this to the Kenyan grid, the authors were able to perform optimal sizing and costing of BESS required to take care of this intermittency. This study, therefore, contributes the following: First, it provides a unique research opportunity to analyze the incorporation of a large BESS system into LTWPP to achieve guaranteed and improved dispatchability. Second, it puts forward an optimized sizing strategy based on BPNN prediction, for calculating the optimal size and cost of BESS which meets all constraints. Finally, the study validates the results obtained and demonstrates the efficiency of this strategy via simulations of different scenarios.

The rest of the article is organized as follows: Section 2 presents a background overview of the literature review and mathematical modelling of the system components. The methodology used and problem formulation are described in detail in Section 3. Section 4 entails the performance analysis of BESS, while Section 5 presents a brief description of the case study. Section 6 provides the simulation results obtained and the accompanying discussions. Finally, the last section gives the conclusion of the study.

2. Literature Review

2.1. Background Overview. A simple time series-based approach for wind power prediction was first developed in 1984 by Brown et al. [10] by utilizing the utility's power curve. Thereafter, systematic investigations have been conducted in the field of predicting wind power or speed produced by WER and this has immensely contributed to the development of numerous techniques as well as reliable and effective tools which have been used with different success rates in various wind farms as proposed and reviewed in [11]. As a result, these accurate prediction tools have been found to yield better unit commitment and scheduling plans, achieve desired control of wind turbines [12], minimize the overall costs of operations, and enhance reliability linked with the increased penetration of wind power into the existing electrical grids [13–15]. The most widely used approaches have been summarized in Table 1. Among all the techniques used, AI techniques, especially neural networks, have emerged to be more accurate and reliable while contrasted with traditional statistical models [12].

Using historical data and ANN modelling, the authors in [17] presented a tool that would be used by operators of RES systems to realize improved management and monitoring of

Table 1: Comparison of different wind forecasting techniques [16].

S. No	Prediction approach	Key features	
		Merits	Demerits
1.	Statistical approaches (e.g., autoregressive (AR) model, moving average (MA) model, autoregressive moving average (ARMA) model, autoregressive integrated moving average (ARIMA) model	(i) No need of expert skill. (ii) Very reliable since it uses the readily available historical weather data. (iii) Very easy to determine the prediction intervals (iv) For short-term predictions, they have proven accurate.	(i) Not possible to perfectly capture the intermittent nature of forecast parameters. (ii) Huge amount of historical input values required by these approaches. (iii) For long-term predictions, they have proven less accurate
2.	Persistence methods	(i) For very short-term predictions, they have yielded high accuracy.	(i) For long-term predictions, the accuracy decreases.
3.	NWP/Physical techniques	(i)Utilizes the physical description of the wind farm site, for example obstacles, orography, etc., to model its conditions (ii) Able to address computational fluid dynamics (CFD) for simulating the atmosphere. (i) Best suited for long-term prediction.	(i) Inapplicable for short-term predictions owing to computational difficulties. (ii) Very challenging to obtain physical data for the input to the model. (i) Much time required due to the intensity of calculations.
4.	Support vector machine-based approach	(i) Considered among one of the best supervised learning algorithms. (ii) Exhibits better generalization capabilities.	(i) Its optimization structure is very complex (ii) The accuracy of the model depends on the correct adjustment of parameters. (iii) Requires longer training time
5.	ANN-based techniques	(i) Applicable in modelling very nonlinear complex relationships and is very sensitive even to the slightest variation in data. (ii) It is a knowledge-based system hence it learns by training and explicit mathematical expressions not required	(i) Requires an optimal training algorithm and a large dataset to train the model. (ii) It could be challenging to design the model. (iii) As the neural network becomes larger, it requires more processing time.
6.	Fuzzy logic techniques	(i) Simple to implement. (ii) Able to handle uncertainties and nonlinearities. (iii) Considered relatively less complex technique for models hard to design precisely. (iv) Rule-based learning betters the accuracy of predictions.	(i) Model becomes complex, hence the increase in computational time. (ii) Exhibits weak learning ability compared to ANN. (iii) Dependent on the expertise and intelligence of humans
7.	Hybrid AI technique	(i) Employs the best characteristics of the above single forecasting techniques to minimize their limitations. (ii) Applied for bigger systems. (iii) Minimizes the risk from extreme events	(i) Difficult to design and train. (ii) Input data should be preprocessed to obtain accurate forecast generalization capability.

their systems. The development of the prognostic tool was able to give an adequate forecasts 8 hours ahead of the absolute minimum, maximum, and mean hourly wind power. For short-term and long-term wind farm prediction, the ANN prediction models developed in [18] using the data mining approach were found to outperform the rest of the models.

Using the input parameters such as generation hours, relative humidity, and mean wind speed, the neural network model developed in [19] offers a reliable indicator for the output power from wind farms. The authors in [20] used ANN technique to approximate the wind speeds at a particular location utilizing the speeds of wind at a strong correlation location among neighboring locations. A wide comparison based on time horizons, performance analysis, and statistical distribution of normalized errors is conducted between five different types of ANN models, ARMA models,

and ANFIS models in [21]. ANN models showed better performance. Local dynamic recurrent neural network models employed in [22] for long-term prediction of wind power and wind speed outshined the static rivals with reference to the improvement gained and forecast errors over the persistent method. The authors in [23] predicted wind speed automatically employing a hybrid neural network approach, comprising a radial basis function neural network (RBFNN) and a self-organizing map (SOM). The results indicated that the suggested method yielded improved output with small error rates.

An in-depth comparison study of three kinds of classical ANN approaches—adaptive linear element (ADALINE), radial basis function (RBF), and feed forward back propagation (FFBP)—is conducted in [24]. Results indicated that different model structures, inputs, and learning rates had a direct effect on the prediction accuracy. An advanced study was performed by the authors in [25] who proposed Bayesian model averaging (MBA) technique to merge the forecasts received from diverse ANN models, namely RBF, BPNN, and ADALINE neural networks. Utilizing their posterior model probabilities, BMA approach weights the individual forecasts. The better performing predictions acquire higher weights than the worse. This approached proved to be effective as shown by the simulation results.

Other various promising approaches for enhancing the accuracy of the prediction models includes: hybridizing different forecasting or numerical weather prediction (NWP) models as discussed in [26–32], filtering of systematic errors emanating from NWPs using Kalman filtering [33], proper selection of input parameters [34], or the combination of any of the abovementioned promising approaches [15, 35]. Nonetheless, hybrid techniques may not at all times outperform the single techniques for all forecasting time horizons investigated as shown by the studies in [27].

Due to its ability to construct complex nonlinear relationships via training, and its ease of construction, ANN has been found to be generally a good choice for wind energy prediction. Most forecasting studies using ANN have offered the best performance compared to other techniques [12]. A more cost-effective option may be to utilize some optimal storage at the wind farm to mitigate the abovementioned problems as depicted by many ongoing studies and projects around the globe [36, 37]. Many researches have employed metaheuristic techniques such as GA, PSO, ABC, or a hybrid combination of AI and evolutionary computation such as ANN-PSO to optimally design and operate RES-based hybrid energy systems.

For instance, in [38], the optimization of an off-grid power system that consisted of the PV, WTG, diesel generator, and energy storage system (ESS) was investigated using GA. The proposed algorithm was found effective to aid the distribution network operators to reduce the total system cost that was related to the operation of a microgrid system. Authors in [39] performed simulations employing GA and the rule-based approach to optimize the cost of operation, while in [40], the authors used the firefly algorithm and considered the BESS's depth of discharge while modelling the BESS operation cost. The cost of operation was well reduced as indicated by the results.

Various strategies have been suggested for obtaining the optimal size of BESS. For instance, a life cycle planning methodology of BESS in an off-grid was put forward in [41]. Using decomposition coordination algorithm, the optimal allocation of distribution energy resource (DER) capacity was carried out to match the demand growth while considering dynamic factors, namely demand growth and components' uncertainties. Authors in [42] used an incremental cost approach to obtain the optimal values of BESS to realize the least running cost for an islanded DC microgrid, while in [43], the authors employed the grasshopper optimization algorithm to size the BESS while considering the energy cost and power supply probability efficiency.

In [44], the study found out that the grid-connected BESS was cheaper to operate than the stand-alone one, hence deserving consideration for efficient dispatch of wind power. Owing to the uncertainty of solar PV and wind, [45] asserted that capacity sizing was vital to completely meet the load demand. They formulated PSO algorithm to determine the optimal size for hybrid wind-PV with BESS while considering the unreliability in solar and wind energy generation.

To improve reliability, reduce cost, and to determine the optimal sizes of RES and BESS for a grid-connected microgrid system, the study in [46] used two constraint-based iterative search algorithms. Authors in [47] used ANN to validate the predicted load model and utilized GA to solve a chance-constrained model that handled the variability linked to RES. The results from the study showed that the storage system plays an essential role in renewable energy integration and in the reduction of environmental pollution.

From the background overview, it could be noted that the integration of RES into the existing large grids is very current and is gaining momentum globally, Kenya included. When a sector is new, there is always room for further studies. WER prediction offers one solution of efficiently integrating intermittent sources into the power grids while BESS acts as another solution as highlighted in the current studies reviewed in this section. Unlike these studies which have majorly employed these solutions independently, this study is unique in that it has employed the strength of both solutions to yield a better and improved way of guaranteeing dispatchability of LTWPP whereby the predicted output of the wind farm is utilized to optimize the BESS.

2.2. Mathematical Modelling

2.2.1. The Wind Turbine Generator (WTG) Model. The power output of WTG is estimated [38] according to the following equation:

$$P_{wtg} = \frac{1}{2}\rho A V^3 C_p \eta_g \eta_b, \tag{1}$$

where ρ is the density of air ($\approx$ 1.225 kg/m^3); V is the free wind speed (m/s); A is the area swept by the rotor (m^2); C_p is the power coefficient (dimensionless), η_g and η_b are generator efficiency (%) and gear or bearing efficiency (%), respectively.

From the WTG profile in Figure 1, the wind power is given by the following equation [44]:

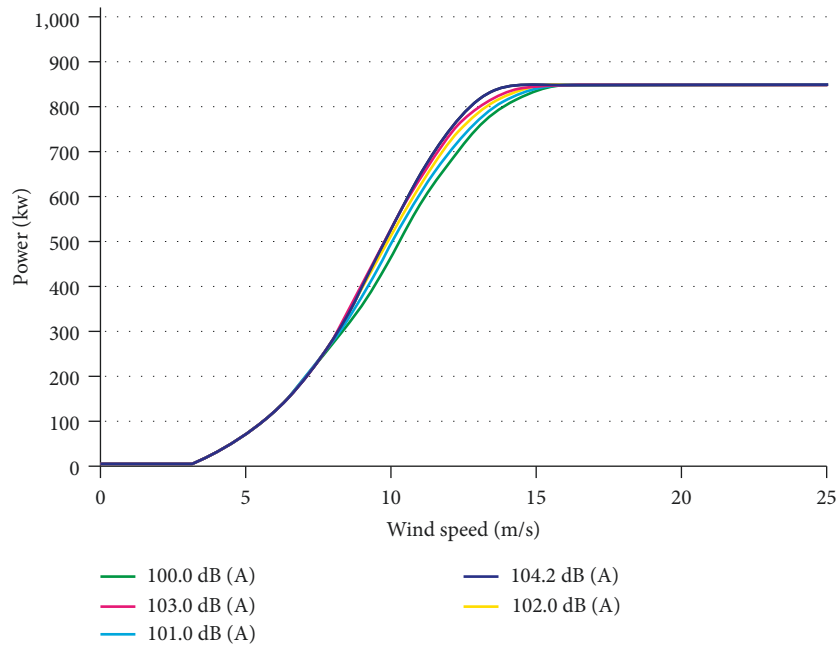

Figure 1: The power curves of V52-850 kW turbine at different sound levels.

$$P_{\text{wtg},t} = \begin{cases} 0, & 0 \le V_{t,s} \le V_{CI} \text{ or } V_{t,s} \ge V_{CO}, \\ P_{\text{wtg}}^{\max} \dfrac{V_{t,s} - V_{CI}}{V_R - V_{CI}}, & V_{CI} \le V_{t,s} < V_R, \\ P_{\text{wtg}}^{\max}, & V_R \le V_{t,s} \le V_{CO} \end{cases}, \quad (2)$$

where $P_{wtg,t}$ represents the wind power produced at time t, $V_{t,s}$ represents the wind speed at any hour t, V_{CI} represents the cut-in wind speed, V_R represents the rated wind speed, and V_{CO} represents the cut-out wind speed.

2.2.2. BESS Modelling. Storing the surplus energy available, P_{balance}, produced by the WER is the first requirement that should be addressed in optimal BESS sizing [48] as shown in the following equation:

$$P_{\text{balance}}(t) = P_{wtg}(t) - P_{\text{load}}(t), \quad (3)$$

where $P_{\text{load}}(t)$ represents the demanded power at any given time t, $P_{wtg}(t)$ represents the predicted output power from WTG at any given time t. The positive value of $P_{\text{balance}}(t)$ indicates that the wind farm produces surplus power, while the negative sign indicates a deficit in demand that the wind farm cannot meet.

The strategy is first to store the available energy from the WTG during hours of higher wind output and discharge the BESS when the output power is less than the demand until the BESS reaches a given minimum state of charge (SOC). The variable SOC(t) at any particular hour is the amount of energy stored in the BESS at that particular instant and is formulated as follows:

$$SOC(t) = SOC(t-1) - \frac{(P_{\text{bess}}(t) \times \Delta t)}{E_{\text{bess}}} \forall t \in T, \quad (4)$$

where $SOC(t-1)$ is the SOC at time $t-1$, $P_{\text{bess}}(t)$ represents the charge or discharge power at time t, E_{bess} represents the BESS capacity, and Δt represents the incremental time for the optimization.

The BESS in this study is modelled based on the SOC and depth of discharge (DOD) limits. Increase in DOD increases the cost of BESS due to more power discharged by the BESS. Cost is a very key factor in the development of BESS. Thus, a cheap BESS would be the most economically feasible. The minimum SOC is given as follows:

$$SOC^{\min} = (1 - DOD)SOC^{\max}. \quad (5)$$

The charging and discharging energies at any given time are given in equations (6) and (7), respectively [49].

$$E_{\text{bess}}^{c}(\text{t}) = E_{\text{bess}}(t-1) + P_{\text{bess}}^{c}(\text{t}).\Delta t.\eta_c, \quad (6)$$

$$E_{\text{bess}}^{d}(\text{t}) = E_{\text{bess}}(\text{t}-1) - \frac{P_{\text{bess}}^{d}(\text{t}).\Delta t}{\eta_d}, \quad (7)$$

where η_d and η_c are the discharge and charge efficacy of the BESS (%), respectively, while $P_{\text{bess}}^{d}(t)$ and $P_{\text{bess}}^{c}(t)$ are the discharged and charged powers, respectively.

The following assumptions are made in the optimal sizing of BESS:

(i) Temperature affects the lifespan of lithium BESS. LTWPP site has a mean temperature 28°C, hence a temperature correction factor of 0.964 will be considered [50].

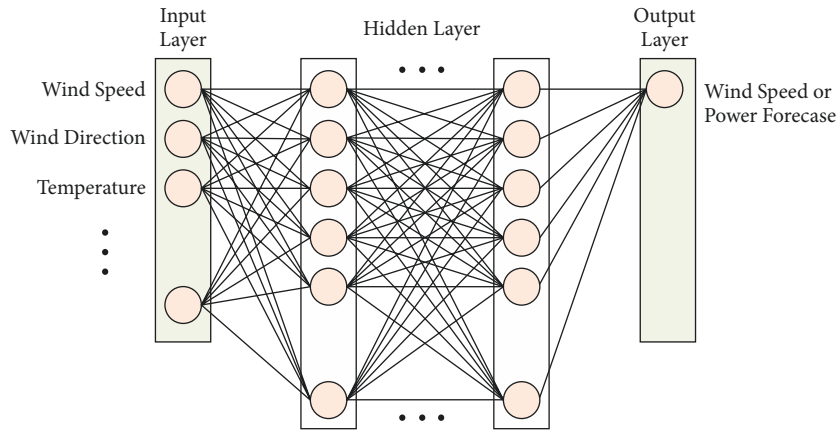

Figure 2: The common topology of a BPNN model.

(ii) As reported in [51], "sudden deaths" of batteries occur when its nominal capacity reaches 80% of its initial value and this usually marks the end of its life. It is for this reason that the aging correction factor of 20% has been selected since the aging process is accelerated after this point.

3. Methodology

3.1. Wind Data Analysis and Preprocessing of the Parameters in LTWPP Farm. First, the data which were obtained from Meteoblue [52] were preprocessed before being applied as a forecast model input. This was for eliminating any sharp peaks or errors in the data and to ascertain that there were not any missing data points. The wind speeds at a hub height of 80 m were then converted to the LTWPP WTG hub height of 44 m using the following expression [53]:

$$v_h = v_o\left(\frac{h}{h_o}\right)^{\alpha}, \tag{8}$$

where v_h denotes the speed of wind at height h, v_o denotes the average speed of wind at h_o, and α denotes the friction coefficient or the Hellman's exponent and is always dependent on the topography at a given site. For our case, α was taken as 1/7 since it is an open land.

3.2. Wind Power Output Prediction Using BPNN. BPNN has two stages in its learning algorithm. First, the training input parameters are fed to the network source nodes and are propagated from one hidden layer to another until the output parameter is produced at the output layer. Second, if the value of this parameter deviates from the anticipated output, an error is evaluated, which is propagated backwards as the network weights are modified. The common structure of BPNN is depicted in Figure 2.

The demerit of utilizing BPNN is its long training duration with very many iterations. To tackle this problem, Levenberg–Marquardt (LM) optimization was employed to train BPNN. Training was performed in batch model. First, the data were normalized. The database was then constructed from the historical real data collected from the LTWPP since it commenced its operation (October 2018 to September 2021).

Data for the first 2 years were used to train and validate the network while the remaining ones for a year, which was used to test the network. The optimum architecture of the BPNN, that is the choice of the optimal number of hidden layers, was performed using a combination of trial-and-error method and the proposed method in [24], where the optimal number of hidden layers (h) is given by the whole number near to log (T), where T denotes the total number of vectors used for training. The training, validation, and testing process of BPNN is illustrated in Figure 3.

The proposed optimal sizing strategy flowchart based on BPNN prediction for evaluating the BESS size and cost is shown in Figure 4.

3.3. Optimal Sizing of Battery Energy Storage System

3.3.1. Selection of BESS. Batteries have so far demonstrated to be an economically feasible energy storage technology. Previously, low round trip efficiency and high costs hampered the mass deployment of BESS. The high efficiency and reduction in cost of lithium-ion batteries led to the surge of BESS usage in the last few years for both large-scale grid-level deployments and small-scale behind-the-meter installations [54]. Table 2 shows the distinguishing characteristics of the various battery technologies currently in the market. It can be clearly seen that Li-ion ranks the best due to the superior characteristics it possesses in comparison to other battery types. The critical review done by [55] indicates that Li-ion batteries as the most suitable and with high potential for RES integration into the power grid. However, their cost still needs to be minimized if they are to be embraced fully. Therefore, this study proposes to use lithium-ion batteries.

3.3.2. BESS Sizing. The daily BESS average energy need, $E_{\text{bessAv.}}$ (MWh/day), depicted below is obtained from $P_{\text{balance}}(t)$, evaluated from equation (3).

$$E_{\text{bessAv.}}(MWh) = \max\left\{\sum_{i=1}^{N} P_{\text{balance}}(t) \times \Delta t\right\}. \tag{9}$$

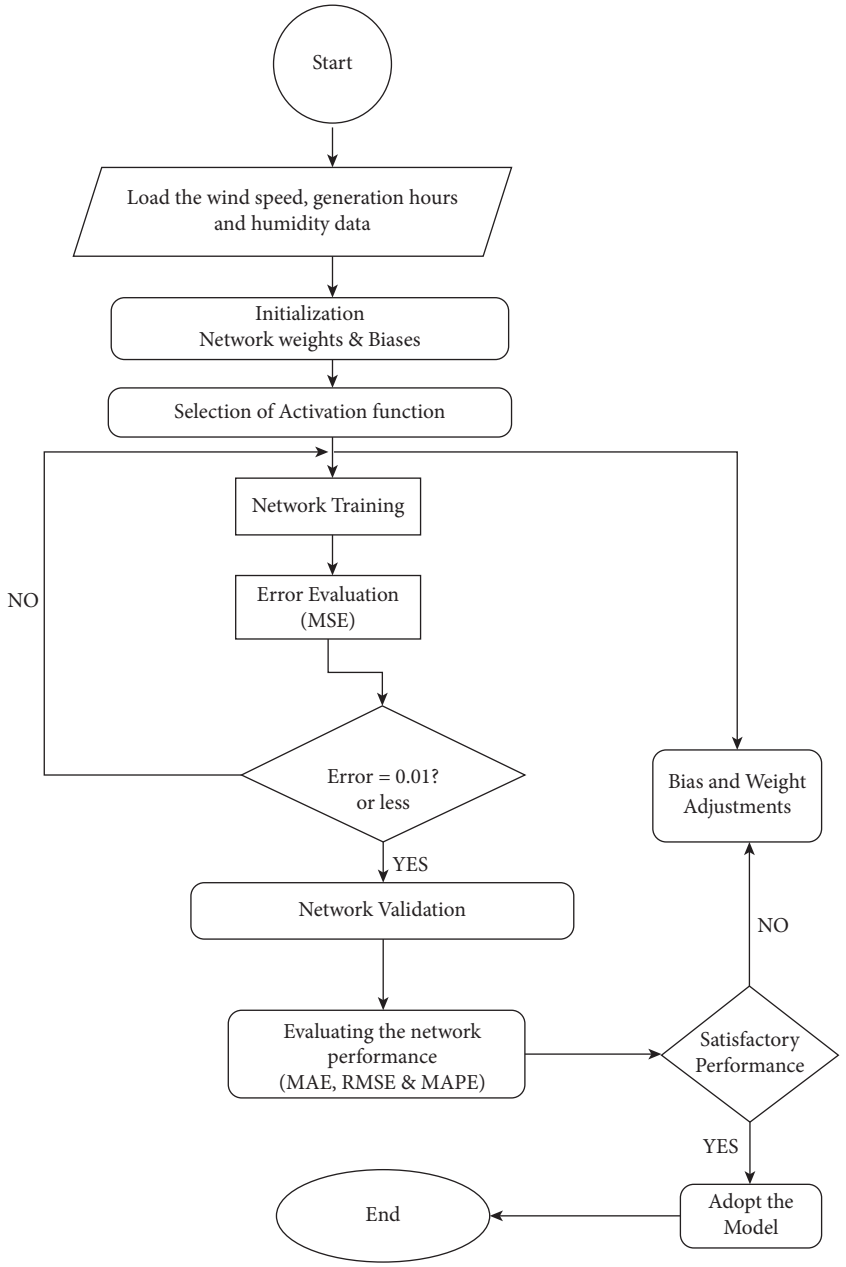

Figure 3: The BPNN training algorithm flowchart.

Based on the considerations and assumptions made in Section 2, the required BESS capacity (MWh) is given by [50];

$$E_{\text{bessmax}} = \frac{Cf \times E_{\text{bessAv.}}\,(MWh/\text{day}) \times D}{DOD\%}, \tag{10}$$

where Cf is the correction factor for the effects of battery aging and temperature degradations and D represents the days of autonomy.

By applying GA, the BESS size obtained in (10) is further minimized with E_{bessmax} used as the maximum boundary limit. GA is a heuristic evolutionary algorithm used for hybrid search and optimization problems. It mimics the Charles Darwin's theory of natural selection [56].

Two of the most notable merits of GA over other optimization algorithms are: parallelism, which helps in false peak reduction [47], and its capability in handling complex problems. It can effectively handle different kinds of optimization, whether the fitness function is linear or nonlinear, or continuous or discontinuous. Nevertheless, GA has few drawbacks. For the fitness function formulation, the choice of critical parameters, namely, crossover and mutation rates, and the selection criteria of the new population must be done carefully, otherwise it will be difficult for the algorithm to converge. GA still remains one of the most widely used techniques in modern nonlinear optimization despite the abovementioned disadvantages [57]. The GA optimization algorithm flowchart is shown in Figure 5.

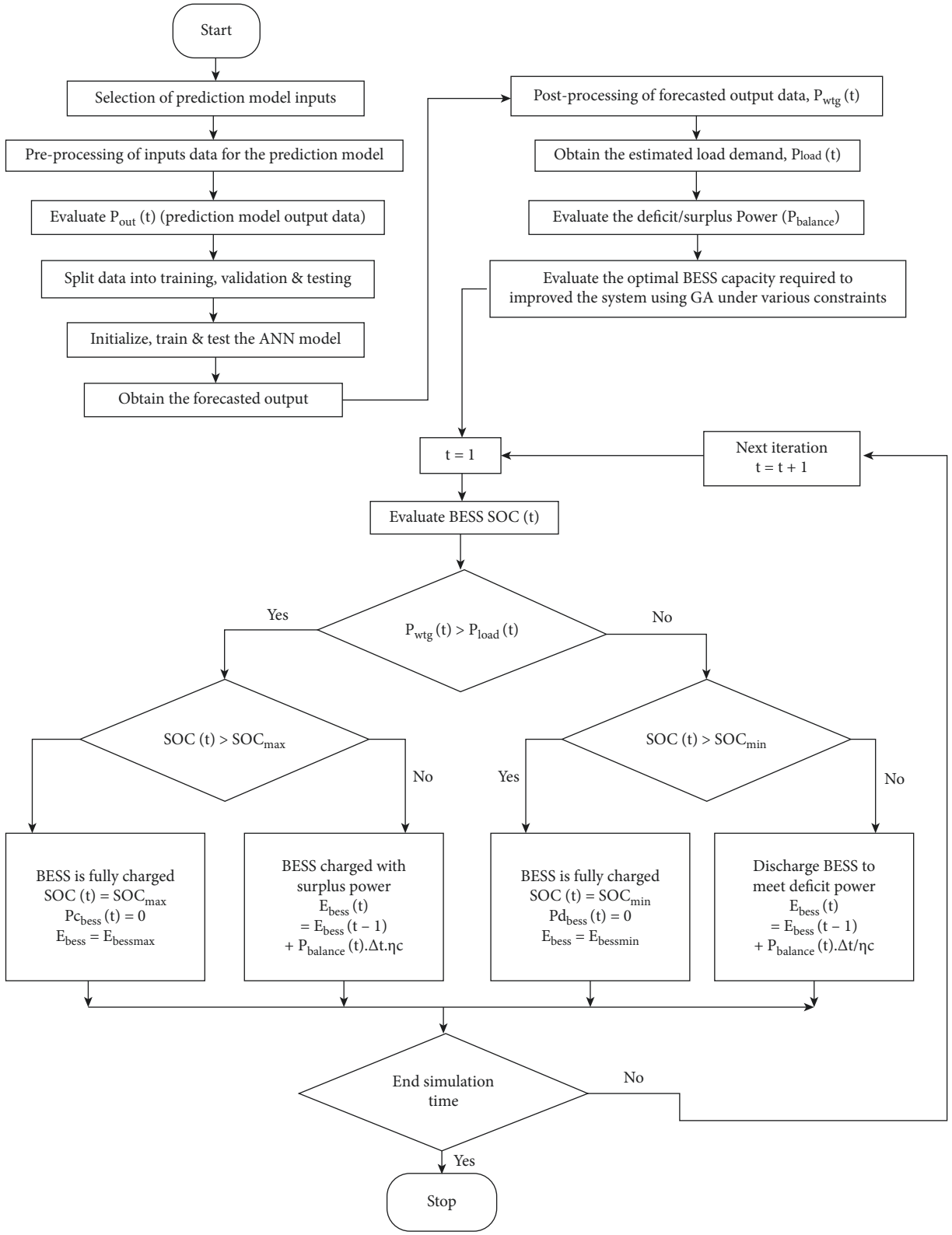

Figure 4: Proposed sizing strategy flowchart.

3.4. Problem Formulation. Stable, efficient, and economical operation of the grid incorporated with WER is largely dependent on the accurate forecasting of the wind power output and optimally sized storage to take care of the uncertainty caused by the variable and intermittent nature of wind. There is a need to optimize WER when it is available. To improve the prediction accuracy of our system, other parameters that affect the wind speed and

Table 2: Distinguishing characteristics of various battery technologies [54].

Time-scale	Power density (kW/Kg)	Efficiency (%) (Round trip)	Lifespan (years)	Environmental friendliness
1. Lithium-ion battery	150–250	95	10–15	Yes
2. Sodium-sulfur (Na-S)	125–150	75–85	10–15	No
3. Redox flow battery (RFB)	60–80	70–75	5–10	No
4. Nickel-cadmium (Ni-Cd)	40–60	60–80	10–15	No
5. Lead-acid battery	30–50	60–70	3–6	No

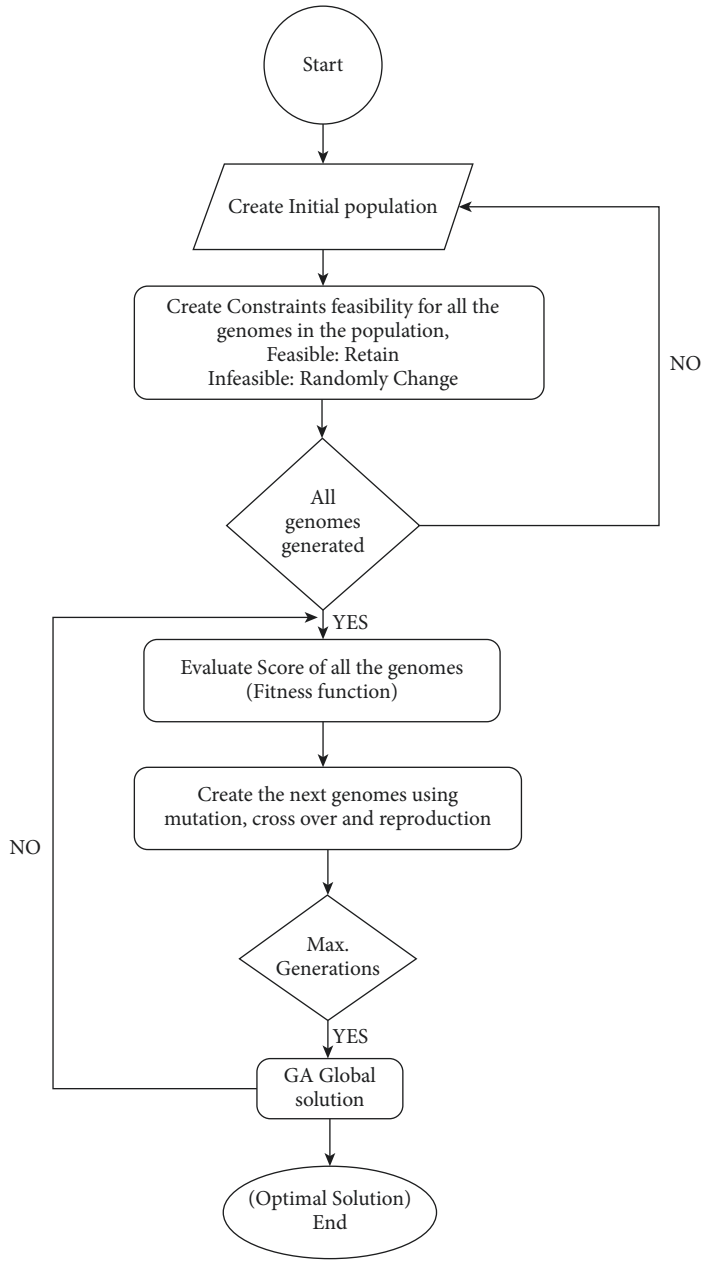

Figure 5: The GA optimization algorithm flowchart.

the average power production by the WTG such as relative humidity, wind direction, and temperature are added as inputs to the backpropagation neural network (BPNN) with Levenberg–Marquardt (LM) optimization technique. The wind power output from the forecast is used to calculate the excess surplus power in equation (3), which is the first key requirement in finding the optimal BESS size.

3.4.1. The Objective Functions. The proposed study aims at sizing an optimal BESS by minimizing the total cost of the lithium BESS investment, when incorporated into grid-connected LTWPP farm, the following equation represents an objective function (OF) to be minimized;

$$\text{Min}\{C_{\text{total}}(E_{\text{bess}})\} = (C_{\text{BESS}} \times E_{\text{bess}}).CRF, \tag{11}$$

$$C_{\text{BESS}} = C_{\text{Cap}}^{\text{BESS}} + r_{\text{BESS}}.C_{\text{Cap}}^{\text{BESS}} + (20 - r_{\text{BESS}} - 1).C_{O\&M}^{\text{BESS}}, \tag{12}$$

where E_{bess} is the storage capacity of BESS in MWh, C_{BESS} is the per-unit cost of the lithium BESS(US$/MWh), $C_{\text{Cap}}^{\text{BESS}}$ is the capital cost of the lithium BESS(US$/MWh), r_{BESS} is the number of BESS replacements, and $C_{O\&M}^{\text{BESS}}$ represents the operation and maintenance cost (US$/MWh). The capital cost consists of the buying, power conversion, and installation costs.

CRF is given equation (13) and represents the capital recovery factor. It enables the calculation of annual payments, which are spread equally over a stipulated time based on the initial payment where n is the BESS lifespan and i is the discounted interest rate.

$$CRF = \frac{i(i+1)^n}{(i+1)^n - 1}. \tag{13}$$

3.4.2. Constraints. The objective function given by equation (11) is subject to:

(1) Balance Constraint. The total demanded power by the users must be equal to the total produced power by the WER and BESS, as depicted in the following equation:

$$P_{wtg}(t) + \text{P}_{\text{bess}}(t) = P_{\text{Load}}(t). \tag{14}$$

(2) BESS Constraints. The power for charging and discharging BESS must be restricted according to the following equations:

$$0 \le P_{\text{bess}}^{c} \le P_{\text{Bessmax}}^{c} = \min\left\{\frac{E_{\text{bess}}^{\max}}{(\Delta t.\eta_c)}, \frac{(E_{\text{bess}}^{\max} - E_{\text{bess}}(t-1))}{\Delta t.\eta_c}\right\}, \tag{15}$$

$$0 \le P_{\text{bess}}^{d} \le P_{\text{Bessmax}}^{d} = \min\left\{\frac{(E_{\text{bess}}^{\max}.\eta_d)}{\Delta t}, \frac{\left(\left(E_{\text{bess}}(t-1) - E_{\text{bess}}^{\min}\right).\eta_d\right)}{\Delta t}\right\}. \tag{16}$$

Moreover, the energy stored must be within $E_{\text{bess}}^{\min}$ and $E_{\text{bess}}^{\max}$ at all times as depicted in the following equation:

$$E_{\text{bess}}^{\min} \le E_{\text{bess}}(t) \le E_{\text{bess}}^{\max} \forall t \in T, \tag{17}$$

$$E_{\text{bess}}^{\min} = (1 - DOD)E_{\text{bess}}^{\max}, \tag{18}$$

where $E_{\text{bess}}^{\min}$ and $E_{\text{bess}}^{\max}$ represents the lowest and highest BESS energy rating, respectively.

The BESS operates within $SOC^{\min}$ and $SOC^{\max}$ as shown in the following equation:

$$SOC^{\min} \le SOC(t) \le SOC^{\max}. \tag{19}$$

(3) WTG Power Limits. The forecasted wind power output is also limited by its rated power as presented in the following equation:

$$P_{wtg}^{\min} \le P_{wtg}(t) \le P_{wtg}^{\max}. \tag{20}$$

(4) Reliability Constraint

$$\text{LPSP} < lpsp_{cr}, \tag{21}$$

with $lpsp_{cr}$ representing the maximum allowed LPSP.

4. The Case Study

LTWPP, the largest wind farm in Africa, is located in Sarima (2.49Â°N 36.8Â°E), between the foot slopes of Mt Kulal and the southeastern end of Lake Turkana, in Loiyangalani District, Marsabit County, Kenya. The area, often labelled as "The windiest place on Earth," has distinct geographical conditions whereby the variations of daily temperature produce strong wind streams between the desert hinterland (with steep temperature variations) and Lake Turkana (with relatively constant temperature). It comprises of 365 Vestas V52, doubly fed asynchronous WTGs, each with a capacity of 850 kW, which generate a total of 310.25 MW of electricity. The technical specifications of the WTGs are given in Table 3. The power generated from the WTGs is transmitted to the wind farm internal overhead electric wires (collection grid) with the voltage of 33 kV via 0.69 kV/33 kV transformers to a sectionalized 33 kV substation that is located within the premises. Through a 33/220 (400) kV substation, the wind farm is AC-connected to the grid via a 400 kV high-voltage double transmission line [60]. Figure 6 shows the topology of the LTWPP incorporated with BESS.

5. Performance Analysis of Battery Storage

5.1. Reliability Model. In sizing BESS, the power reliability analysis is very crucial. When the energy generated by WTG plus the energy stored in the BESS fails to meet the load demand at hour t, the system experiences loss of power supply (LPS) [49] and is expressed in equation (22) as;

Table 3: System parameters.

System model	Parameter	Value
1. V52-850 kW WTG data [58]	Rated power output:	850 kW
	Rotor diameter swept area by the rotor	52 m
	Cut-in wind velocity	2,124 m^2
	Nominal wind velocity	4 m/s
	Cut-out wind velocity	16 m/s
		25 m/s
2. Li-ion BESS data [50, 59]	The capital cost	$ 0.469/wh
	Maintenance and operation cost	$0.000115/wh
	Total life cycles	3500 cycles
	DOD	80%
	Charge efficacy	99%
	Discharge efficacy	95%
	Total charge/discharge lifecycles	3500

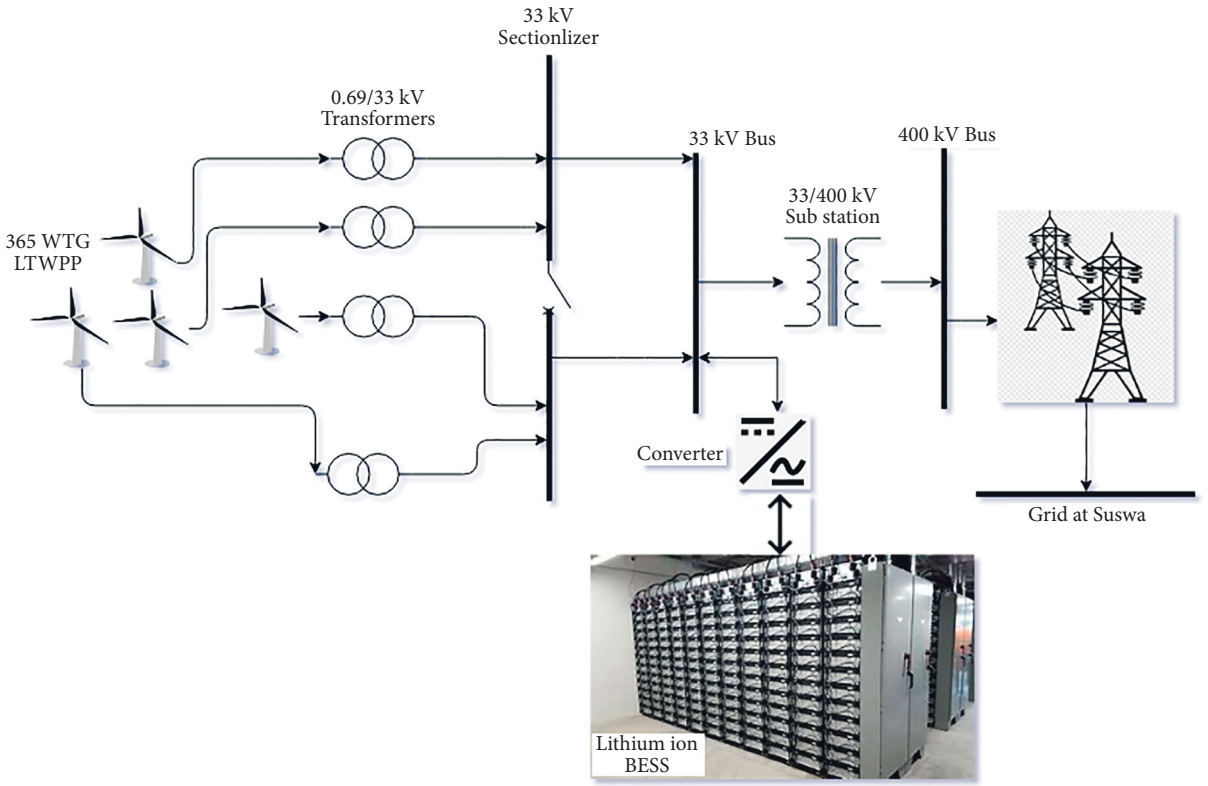

Figure 6: The topology of the LTWPP incorporated with BESS.

$$LPS(t) = P_{\text{load}}(t) - \left[P_{wtg}(t) + P^{d}_{\text{bess}}(t)\right].\eta_{\text{inverter}}, \tag{22}$$

where η_{inverter} is the efficiency of the inverter.

Using LPS, the loss of power supply probability (LPSP) is evaluated as follows [9]:

$$\text{LPSP} = \frac{\sum_{t=1}^{T} LPS(t)}{\sum_{t=1}^{T} P_{\text{load}}(t)}. \tag{23}$$

The key aim in sizing BESS is to ensure that LPSP $< lpsp_{cr}$ which is 0.1 in this study.

5.2. Power Shed. When $P_{wtg} < P_{\text{load}}$, it necessitates load shedding in order for the RES without storage to match the dispatch curve. Alternative sources of energy such as diesel generators are usually assumed to cater for this deficit power. Thus, the revenue loss due to power shed, RL_{shed}, is given by the following equation [50]:

$$\begin{aligned} P_{\text{shed}}(t) &= P_{\text{load}}(t) - P_{wtg}(t), \\ RL_{\text{shed}} &= \sum_{t=1}^{T} P_{\text{shed}} \times C_{\text{diesel}} \times t, \end{aligned} \tag{24}$$

where C_{diesel} is the cost of diesel generators and is estimated to be US$ 0.27/KWh of electricity.

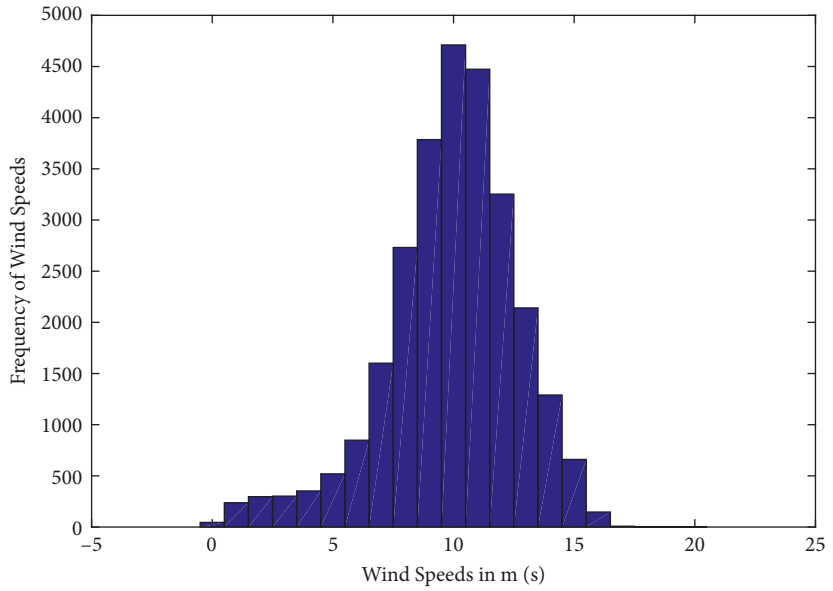

Figure 7: LTWPP windspeed histogram.

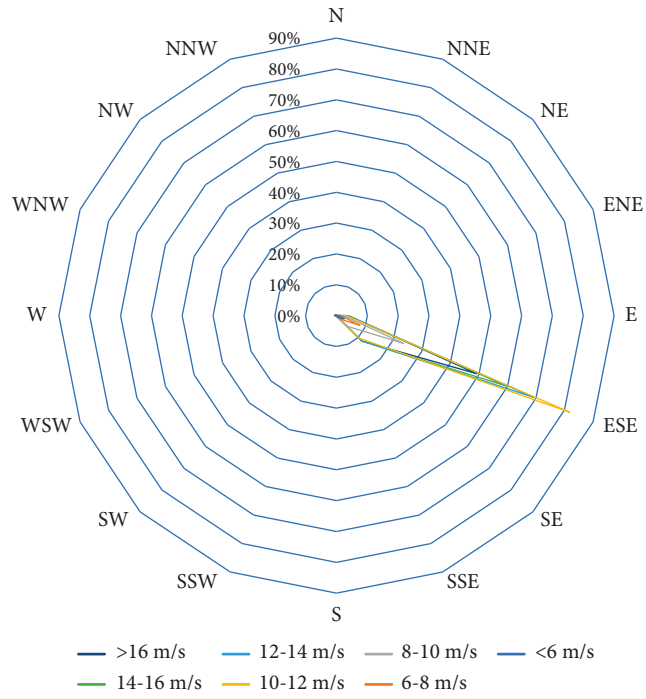

Figure 8: A wind rose for LTWPP farm.

6. Simulation Results and Discussion

Figure 7 is a representation of the histogram of various wind speeds at LTWPP from 01/09/2018 to 15/09/2021. The average value of the collected hourly wind speeds was between 10.5 and 11.5 m/s. Weibull parameters for the above data were found to be scale factor, c = 10.9096 and shape factor, $k = 4.1525$. The wind rose of LTWPP with 16 directions is represented in Figure 8. It can be deduced that the dominant wind which averages at 11 m/s blows from ESE direction. The data obtained from Meteoblue [52] were found to be good for usage since there were no missing data for the period under study as shown in the relative humidity, ambient temperature, wind speed data, and the calculated output power in Figure 9. In addition, the data were within the normal expected range and the overall pattern and mean are the same as the ones found in the literature [61].

The BPNN training performance results are tabulated in Table 4. The best performance MAE, MSE, and RMSE were

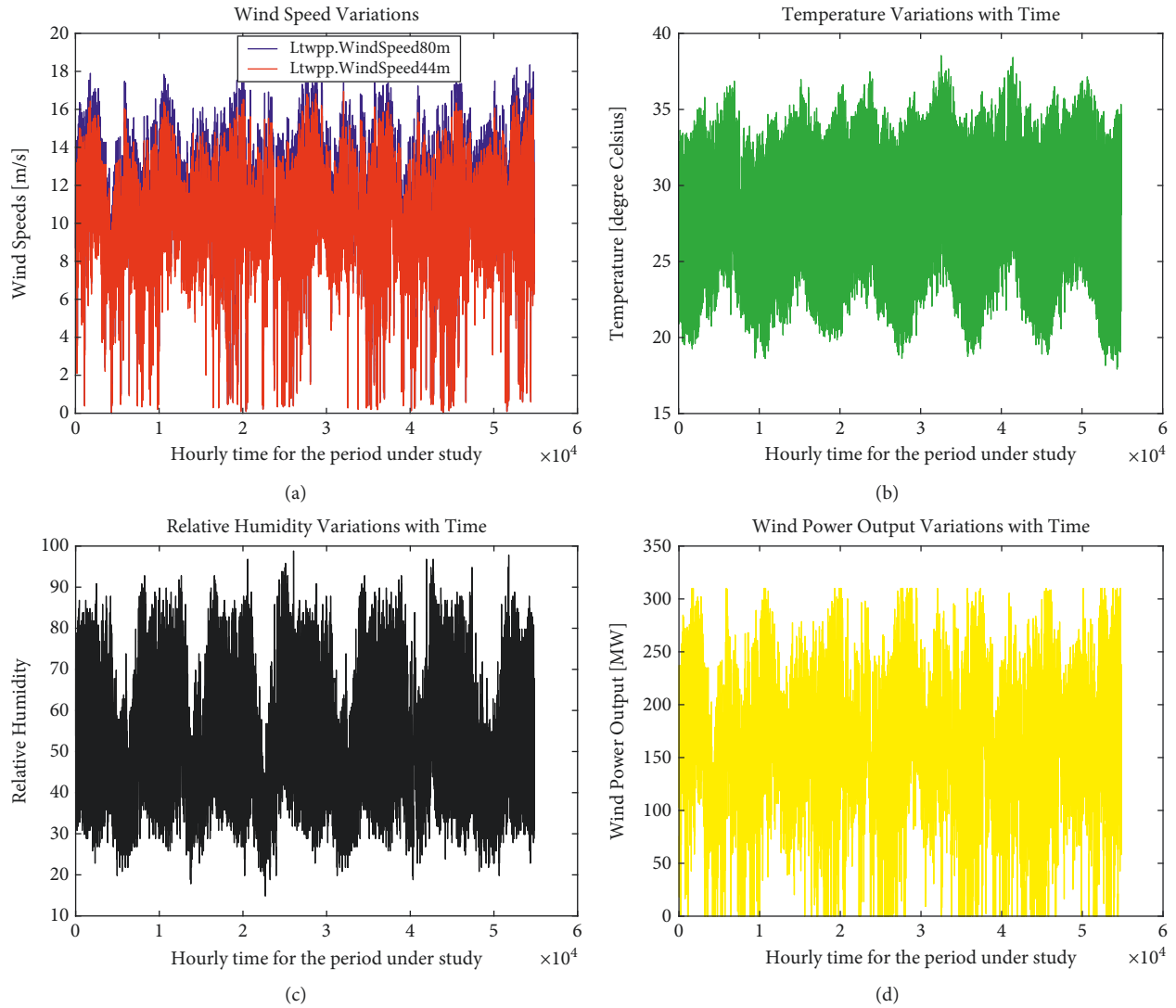

Figure 9: Preprocessed wind data for the time period under the study.

found to be 2.29×10^{-5}, 2.35×10^{-5}, and 4.85×10^{-5}, respectively.

The regression and performance plots for the BPNN training are depicted in Figures 10 and 11(a), respectively. Results on Figure 11(b) indicates the effectiveness of the proposed algorithm in forecasting the output wind power of LTWPP since the predicted power output curve is almost the same as the actual power output curve. This neural forecasted output is used in the optimal sizing of the BESS.

The average per hour daily load demand to be supplied by LTWPP is given in Figure 12, while the hourly data for the 12 months used in this study is shown in Figure 13 for the period between October 2018 and September 2019. As it stands now, there is no specific amount of demand that is allocated to LTWPP. Instead, it is supposed to supply all power that it generates at any time. However, this poses a challenge to the system in terms of economical dispatch scheduling of other sources since either the geothermal or diesel generators have to be in standby mode to cater for any shortage unmet by LTWPP. In addition, the sudden ramping up or down of these standby sources causes mechanical stresses, hence reducing their longevity.

Therefore, with the incorporation of BESS to LTWPP, it can be able to supply a specific allocated amount to the grid. Any fluctuations of the wind are taken care of by the BESS, hence guaranteeing its dispatchability. This study assigns LTWPP to supply 17% of the total demand on the grid. This arises from the fact that LTWPP contributes an average of approximately 17% of the total demand on the Kenyan grid.

The variations in the predicted supply and demand allocated to LTWPP for a period of 1 year and for 1 day (11 April, 2019) are depicted in Figure 14. It is from these curves that the excess/deficit power that needs to be stored/discharged in the BESS is obtained. From the daily curve, it could be clearly seen that the power demanded in the very early hours of the day when people are still asleep is less than that produced by the LTWPP. However, when it is most needed during the day, especially between 0900 and 1600 hrs, enough is not produced. Thus, from the curves, we can deduce that without storage, we cannot guarantee the dispatchability of the power supplied to

Table 4: BPNN training performance results.

Activation functions in the input, hidden and output layers, respectively	Performance parameters	Number of hidden layers, h					Overall comment on performance
		Log (T)	4	8	15	20	
1. "Logsin" "tansig" "purelin"	MAE	2.39×10^{-5}	7.65×10^{-4}	2.98×10^{-5}	2.61×10^{-5}	1.59×10^{-4}	Excellent compromise between speed and performance
	MSE	6.32×10^{-9}	2.49×10^{-6}	6.65×10^{-9}	1.15×10^{-8}	4.59×10^{-7}	
	RMSE	7.95×10^{-5}	0.0016	8.16×10^{-5}	1.07×10^{-4}	6.78×10^{-4}	
2. "Tansig" "logsin" "purelin"	MAE	4.94×10^{-5}	2.97×10^{-4}	9.45×10^{-6}	1.84×10^{-5}	6.06×10^{-5}	Faster but poor performance
	MSE	1.75×10^{-8}	7.26×10^{-7}	3.26×10^{-9}	6.73×10^{-9}	2.26×10^{-8}	
	RMSE	1.32×10^{-4}	8.52×10^{-4}	5.71×10^{-5}	8.20×10^{-5}	1.50×10^{-4}	
3. "Tansig" "tansig" "purelin"	MAE	2.29×10^{-5}	1.46×10^{-4}	4.14×10^{-4}	2.16×10^{-5}	2.50×10^{-4}	Longer training but best performance
	MSE	2.35×10^{-9}	6.66×10^{-8}	9.48×10^{-7}	9.29×10^{-9}	6.73×10^{-7}	
	RMSE	4.85×10^{-5}	2.58×10^{-4}	9.74×10^{-4}	9.64×10^{-5}	8.20×10^{-4}	

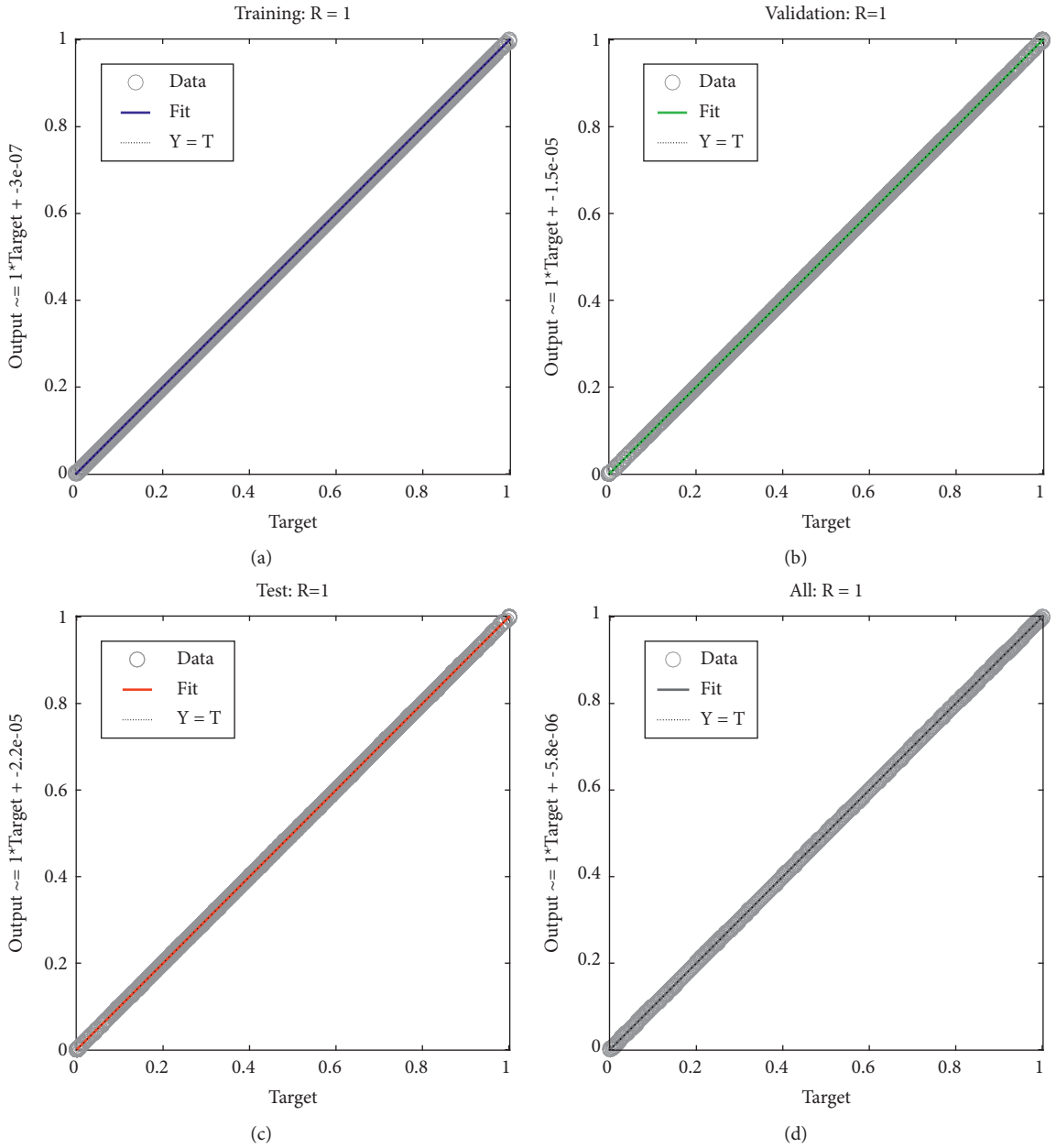

Figure 10: Regression plots for the BPNN training, testing, and validation.

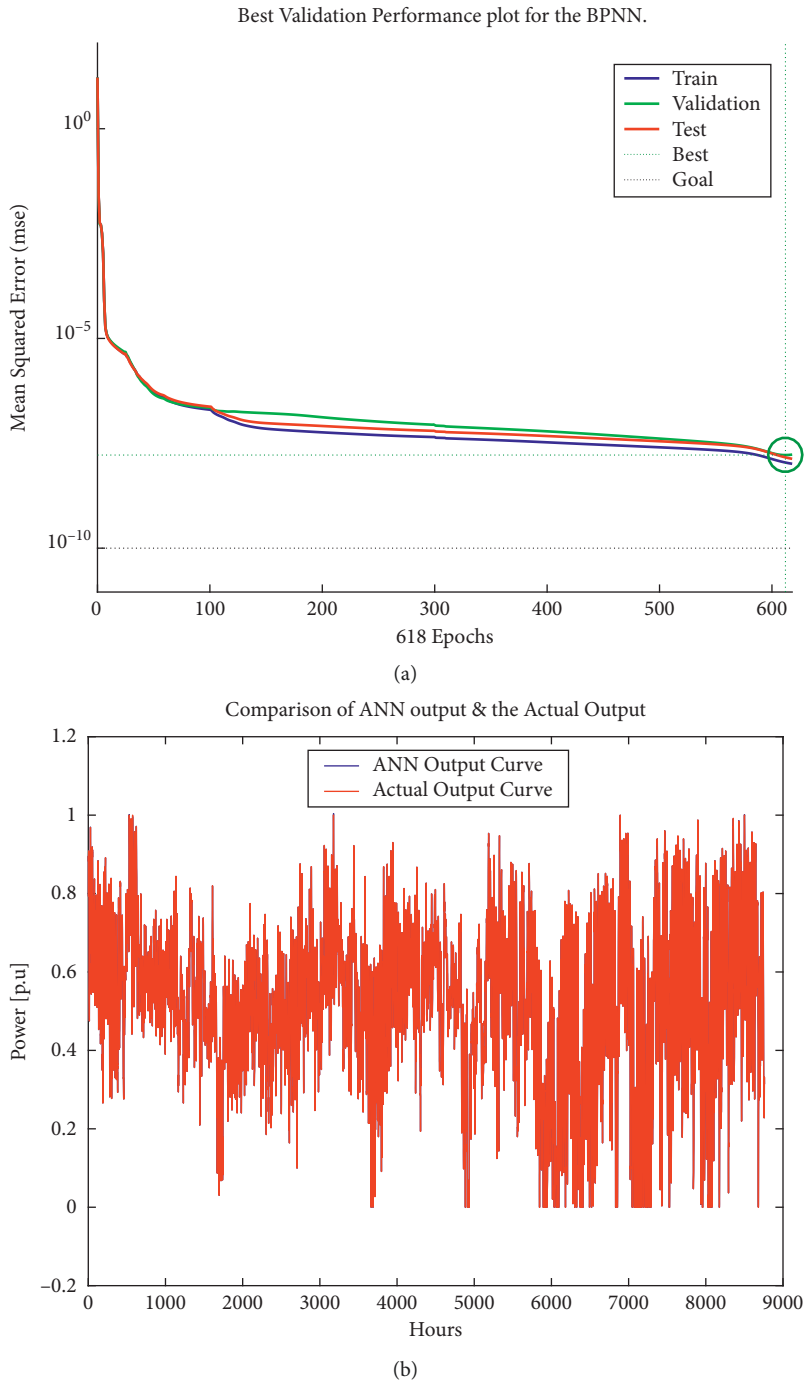

Figure 11: (a) Best validation performance plot for the BPNN. (b) Wind power forecasting performance.

meet the load demanded. The system revenue losses resulting from power shedding amount to a sum of US$ 67,179,299.73 annually with a LPSP ratio of 17.44%.

The size and total lithium BESS cost required are evaluated using equation (10), and the results are tabulated in Table 5. By applying GA, the BESS size obtained in (10) is further minimized with E_{bessmax} used as the maximum boundary limit. The GA parameters that provide the optimum performance are depicted in Table 6. Table 5 also gives the results obtained after optimization.

Optimization of the BESS yielded remarkable changes in the investment costs of the system. The size is reduced to 19.65% of the BESS size evaluated using equation (10). The BESS size thus evaluated is approximately 14.31% of the rating of the LTWPP. These results, based on the proposed methodology, are found to be consistent and, in some instances, better compared to the ones got from previous studies. In a feasibility study conducted in [62], the authors suggested a BESS capacity of approximately 24% of the capacity of PV-wind system. The BESS size obtained

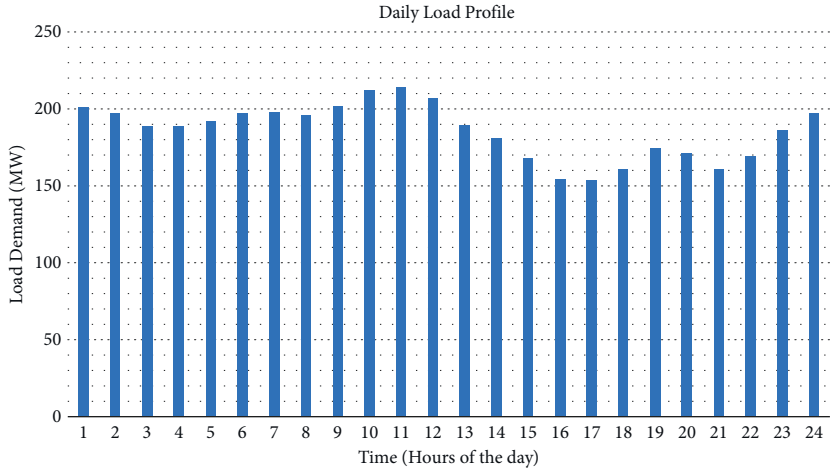

Figure 12: Average daily load demand profile.

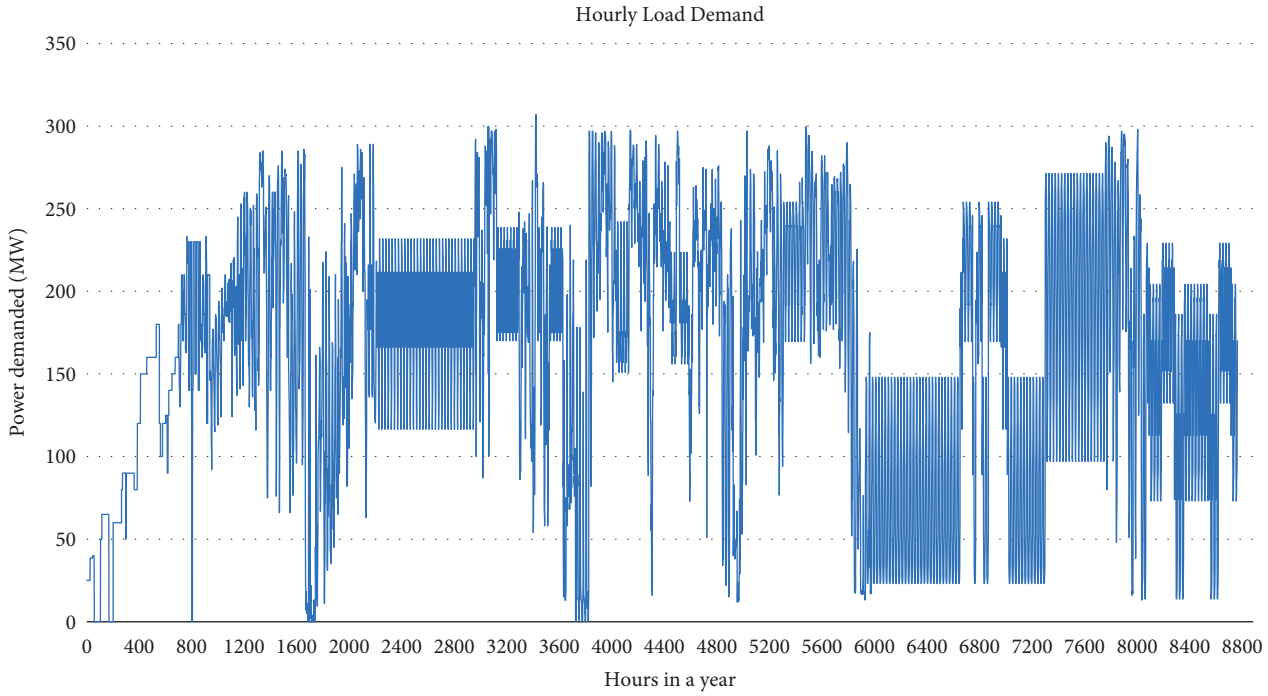

Figure 13: The hourly load demand in a year allocated for LTWPP.

utilizing optimization was 6–10% according to [63], while in [64] the battery size of 15–25% of hybrid RES size is proposed to be adequate for dispatching power effectively. And according to the study carried out in [65] using fuzzy and neural controllers, the BESS size was estimated to be 30–34%. Hence, a BESS of smaller size about 14.31% is proved to be sufficient in this current study.

Gains realized and energy dispatched before and after incorporating BESS with the LTWPP are contrasted. BESS aided to improve the power dispatched by 14.47%, therefore making it possible for the LTWPP to meet the planned dispatch curve for most of the times, thus decreasing the LPSP to 0.0986, which is below the reliability index, LPSP of 0.1. Losses due to power spillage are reduced considerably and hence, the energy saved is used to meet the demand when wind is unavailable. It is worth noting that the power delivered matches the load curve after the incorporation of BESS as shown in Figure 15. Moreover, the feed-in tariff rate for wind power in Kenya is fixed (at US$ 0.11). Thus, any gains earned are as a result of the reduction in power losses through spillage and shedding.

For the period under simulation, the total power discharged to the grid from the BESS is 73406.16 MW. This presents a contribution of 20.52% of the total power supplied by the LTWPP-BESS system. Plots in Figure 16 show the variation of SOC of the BESS with time for a period of 2.5 days. Figure 17 depicts the charging and discharging BESS power. During charging, the BESS power is positive while it

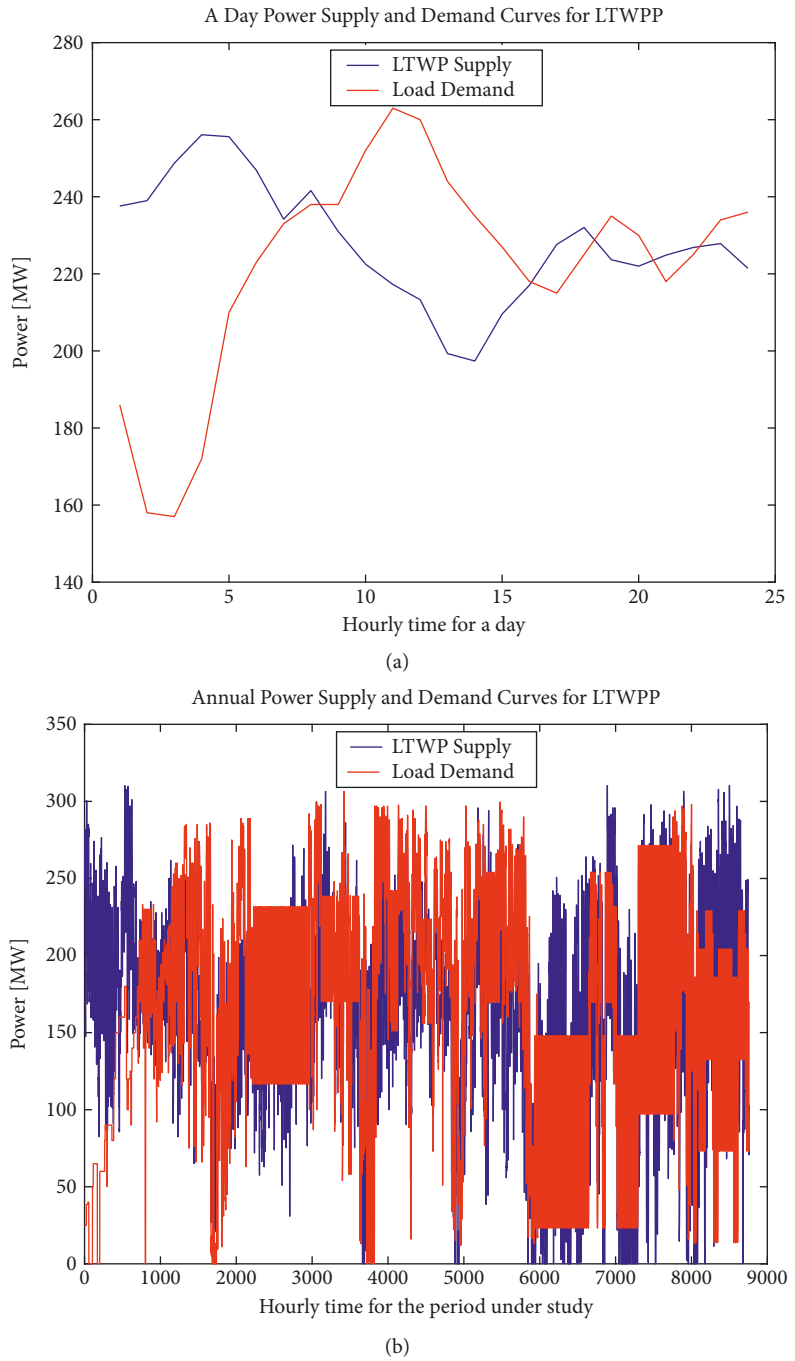

Figure 14: A 1-day (a) and an annual (b) supply and demand curves for LTWPP.

Table 5: BESS sizing without and with optimization.

Type	Capacity in MWh	Investment cost in US$
Lithium-ion BESS	BESS sizing without optimization 903.6676	84,601,948.21
Lithium-ion BESS	BESS sizing with GA optimization 177.5913	16,626,212.98

Table 6: GA parameters.

Parameter	Value
1. Maximum iterations	100
2. Population size, Pop	1000
3. Cros over rate, nc	0.7
4. Extra range factor for crossover, γ	0.4
5. Number of offspring	$nc \times Pop$
6. Mutation rate, nm	0.1
7. Number of mutants	$nm \times Pop$

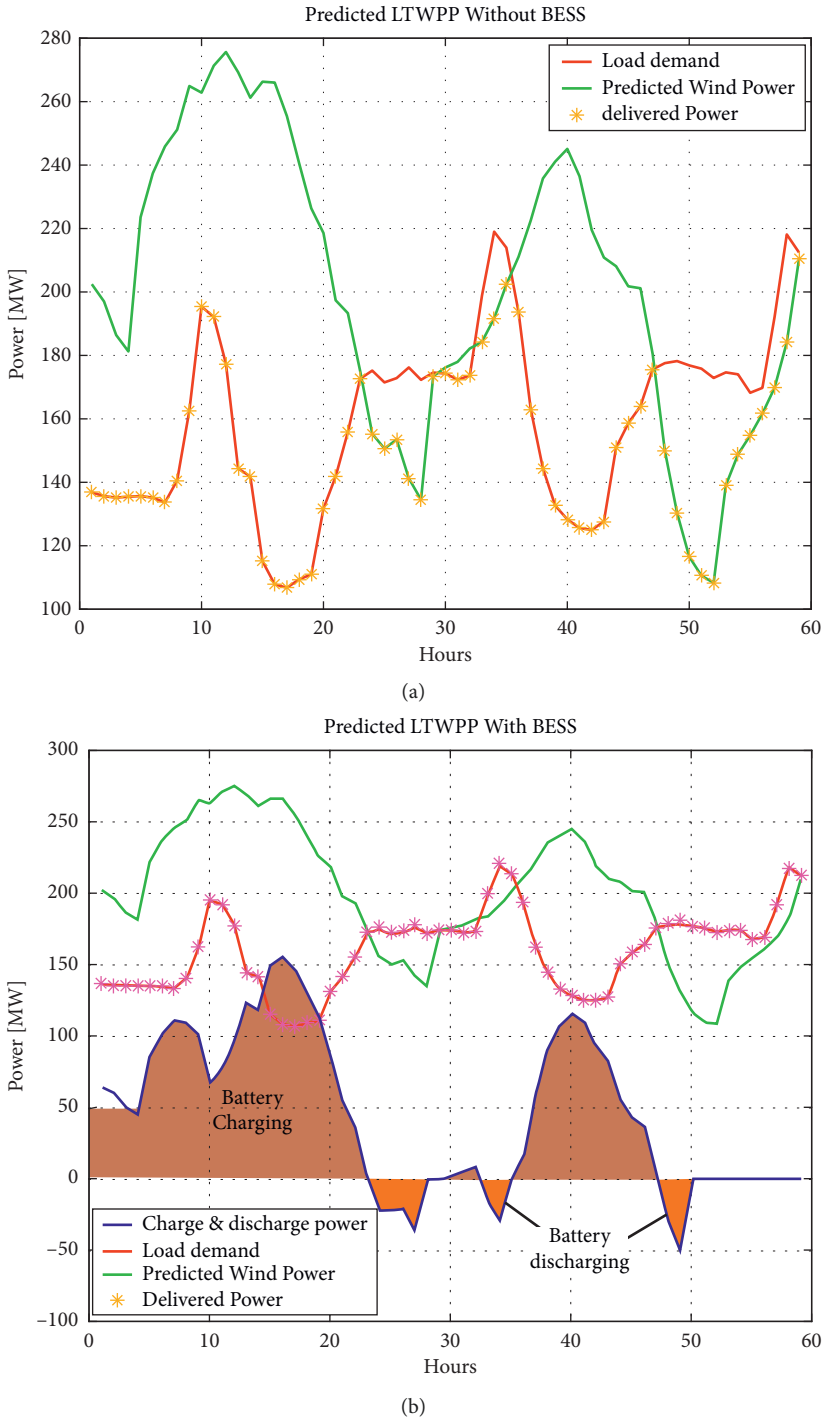

Figure 15: (a) Predicted LTWPP output power without BESS. (b) Predicted LTWPP with BESS.

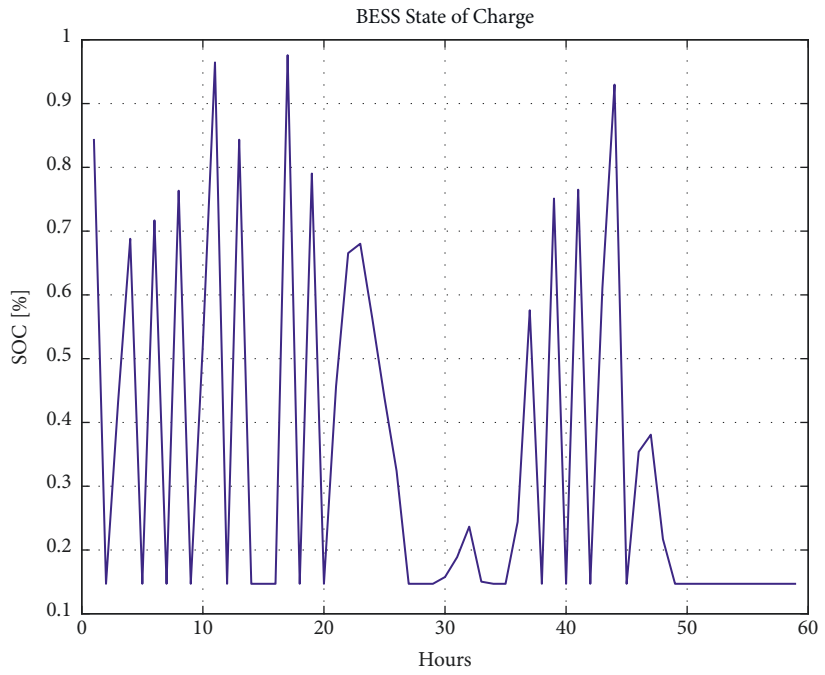

Figure 16: Variation of SOC of the BESS with time.

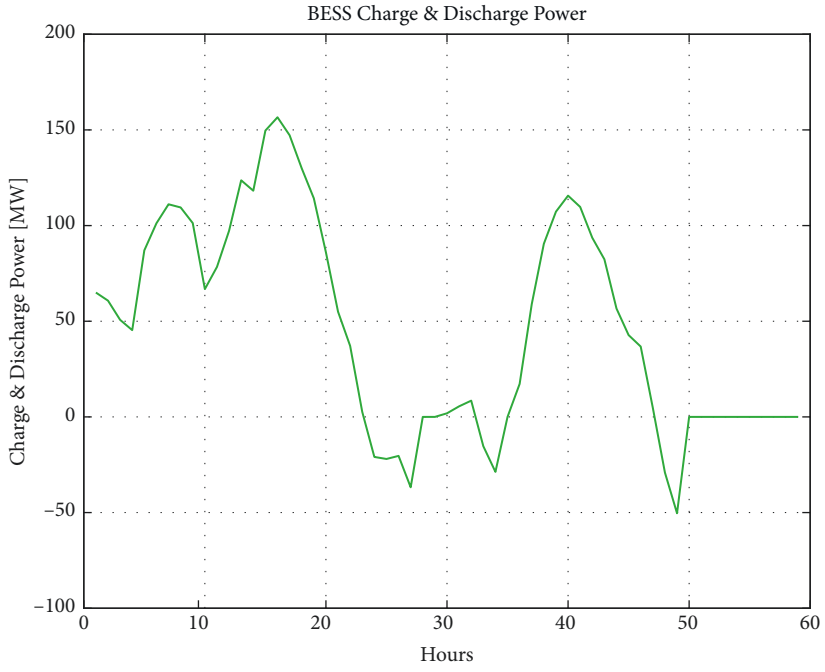

Figure 17: The BESS charge and discharge powers.

becomes negative during discharging. The SOC varies within 98–19.6% limits. This demonstrates the effective usage and performance of the BESS.

The lifespan of any BESS largely depends upon the number of discharge/charge cycles it performs. This was determined to be approximately 300–350 cycles/year. Consequently, the lifetime of lithium-ion BESS in this study is calculated to be approximately 10 years since the total life cycles of the lithium-ion BESS is 3500 cycles. This result shows a better lifetime operation compared to those performed elsewhere. For instance, according to [66], the battery life is estimated to be 2–10 years using a battery dispatch strategy developed to maximize its lifetime. Therefore, this sizing strategy yields an optimal usage of BESS that ensures better dispatchability of LTWPP. To further demonstrate how effective the proposed methodology is, a contrast based on investment cost among diverse possible solutions is shown in Table 7.

Table 7: Comparison of different cases.

Case scenarios	Description	Capacity in MWh	Investment cost in US$	Dispatchability of LTWPP (%)
Case 1a	LTWPP (no forecasting) with no BESS	—	102,634,351.63 (revenue loss incurred due to load shedding)	73.36
Case 1b	Neural prediction of LTWPP with no BESS	—	67,179,299.73 (revenue loss incurred due to load shedding)	82.56
Case 2a	LTWPP (no forecasting) with BESS (no optimization)	1273.5096	119,239,941.70	78.26
Case 2b	LTWPP (no forecasting) with BESS optimization using GA	442.7888	41,458,745.73	72.97
Case 3	Neural forecasted LTWPP without BESS optimization	903.6676	84,601,948.21	94.06
Case 4a	Neural forecasted LTWPP with BESS optimization using GA	177.5913	16,626,212.98	90.14
Case 4b	Neural forecasted LTWPP with BESS optimization using PSO	177.5912	16,626,212.98	90.14

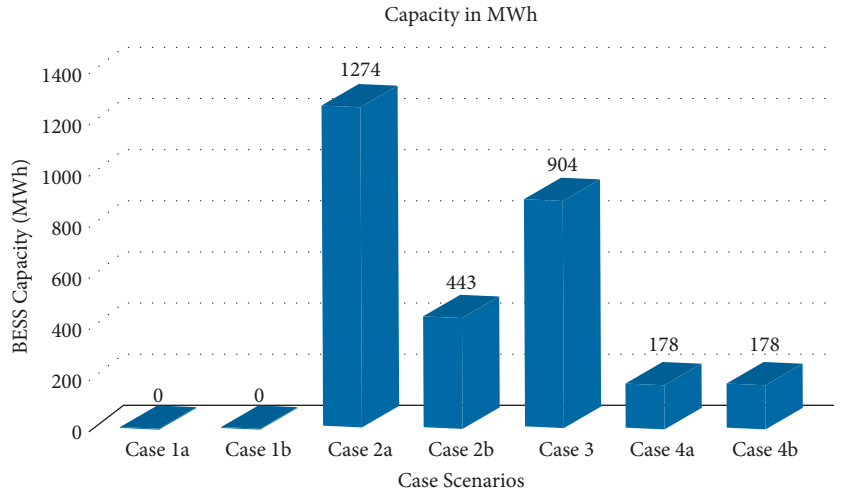

Figure 18: Comparison of BESS sizes under different scenarios.

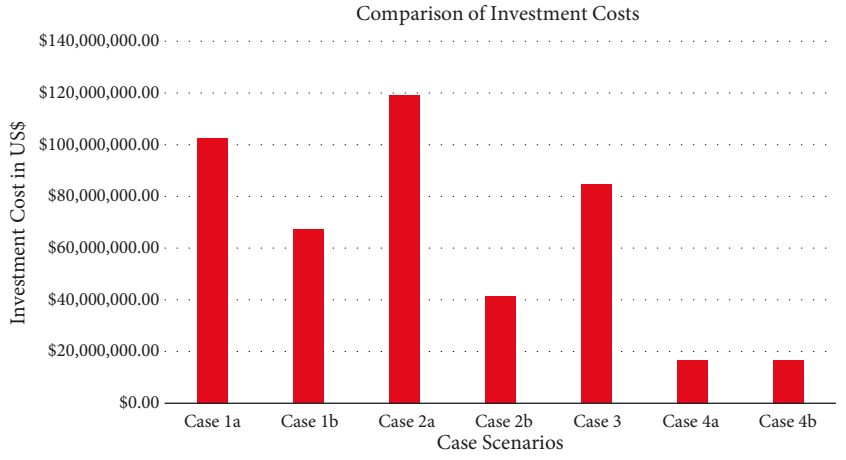

Figure 19: Comparison of investment cost under different scenarios.

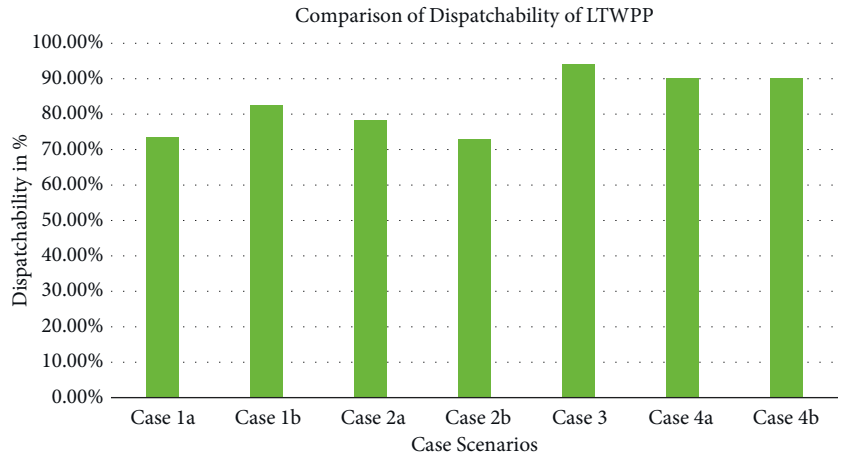

Figure 20: Comparison of dispatchability of LTWPP under different scenarios.

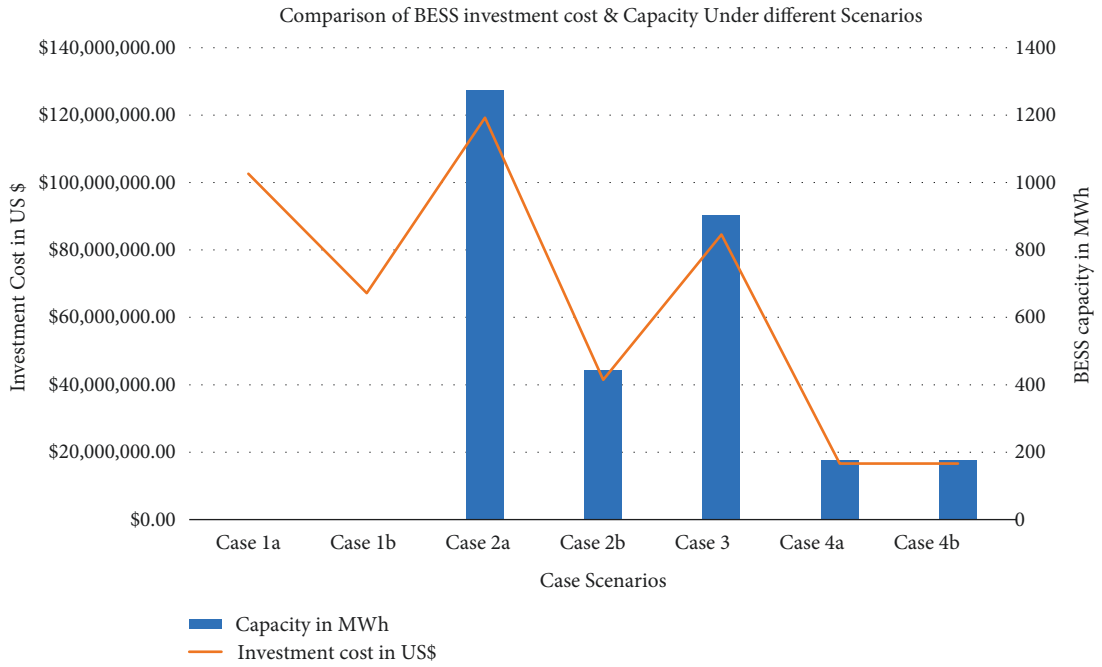

Figure 21: Comparison of BESS capacity and investment costs.

Case 1: (a) and (b) represent LTWPP with no BESS. The second cases represent LTWPP with no forecasting but with BESS. Case 3 represents neural forecasted LTWPP with unoptimized BESS while the final cases represent neural forecasted LTWPP with BESS optimization using both GA and PSO. For the cases of LTWPP with no forecasting, the assumption made was to take the previous year data (October 2017 to September 2018) and use it as the estimate for the period October 2018 to September 2019. From the results in Table 3, various analyses were conducted as illustrated in Figures 18–22.

It can be noted that BESS optimization is very critical as depicted in Figure 18. Optimization reduces the BESS capacity for non-forecasted LTWPP and the neural predicted LTWPP by 65.28% and 80.35%, respectively. This has a direct effect on the investment cost as illustrated in Figure 21. The BESS calculated without optimization and without any prior forecasting of wind power exhibits the highest investment cost, while the neural forecasted LTWPP with BESS optimization exhibits the lowest cost.

Wind energy prediction also plays a very critical role. First, the dispatchability of LTWPP to meet its scheduled demand is found to be generally low for all cases without wind power forecasting as shown in Figure 20. In addition, for Case 1, the neural prediction amounted to a reduction of revenue losses incurred due to load shedding by 34.55% and improved on the dispatchability of the wind farm by 9.2%, without considering any storage as illustrated in Figures 19 and 20, respectively. Furthermore, comparing Case 2a with Cases 4a and 4b, it is found that BESS optimization with

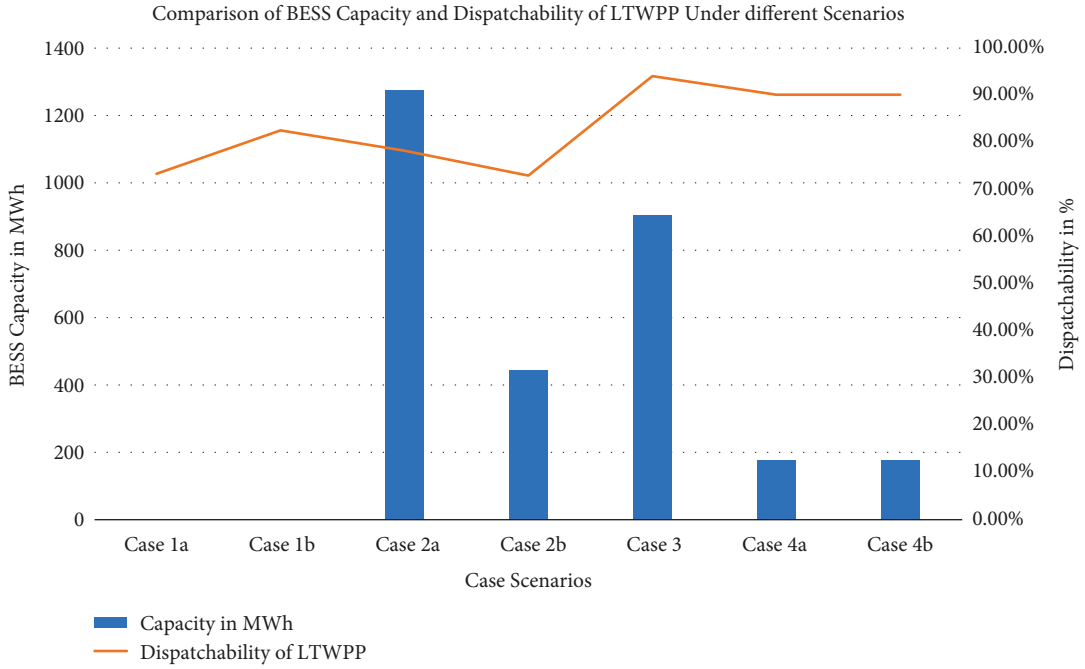

Figure 22: Comparison of BESS capacity and dispatchability of LTWPP.

neural prediction reduces the BESS capacity and investment costs by 59.82%, while improving the dispatchability of LTWPP to 90.14% from 72.97% (Figure 21).

As demonstrated in Figure 22, neural forecasting and BESS incorporation has a direct effect on the dispatchability of LTWPP. It could be seen that the highest dispatchability (94.06%) occurs when we have the prediction of wind together with the large unoptimized BESS capacity. However, the investment cost for this case is very high. Therefore, the optimum dispatch (90.14%), although lower, meets the allowable reliability index of 0.1 and realizes a well-minimized investment cost. This way, by managing the surplus energy through optimizing its storage, the dispatchability of the neural predicted WTG system is improved by 16.78%.

7. Conclusion

Kenya is set for a remarkable growth in the renewable energy sector. This study has suggested an optimized sizing strategy based on BPNN prediction. To effectively minimize the cost of the BESS, the optimization uses a genetic algorithm. Based on different scenarios, performance metrics were analyzed to explore the viability of the LTWPP-BESS system, a grid-connected RES. Due to uncertainties in wind power, BPNN prediction employed improved reliability of the system by improving its dispatchability by 9.72%. A better performance, that is dispatchability improvement of 16.78%, was obtained by utilizing both the predicted output of LTWPP and optimized storage. Moreover, this study found that BESS optimization with neural prediction reduces the BESS capacity and investment costs by 59.82%. LPSP is reduced from 17.44% to 9.86%, while overall dispatchability of LTWPP is increased from 73.36% to 90.14%, hence enabling the farm to meet its LPSP index while guaranteeing dispatchability. Simulation results indicated the sizing methodology based on the BPNN forecasting and dispatch strategy to be effective and efficient since congruous and better results were achieved, in comparison to other previous studies and different scenarios investigated herein.

However, the study did not attain 100% dispatchability, implying that there is still room for further improvement. This could be explored further in future comparative studies using other AI and metaheuristic technique combinations such as ANN-fuzzy and PSO, ANFIS and hybrid ABC-PSO, among many others, which have not been covered in this study. Investigations on the impact of climate change on WER prediction is also of great interest. This proposed research did not include such and could also be included in advancing this study. Inclusion of other key factors that affect the BESS, such as temperature and capacity fade in the constraint, which were excluded in this study, could also be considered. Lastly, future studies should test the designed LTWPP-BESS system on the Kenyan power grid or the equivalent standard IEEE system to evaluate its impact on various power qualities and stability issues.

Data Availability

The data are available upon request from the corresponding author.

Conflicts of Interest

The authors declare that there are no conflicts of interest with regard to the publication of this article.

Acknowledgments

The authors acknowledge the support provided by the African Union Commission in funding this work. They also thank Meteoblue for providing LTWPP site data that greatly aided in conducting this research.

References

[1] Ministry of Energy, "Updated least cost power development plan, 2011-2031, energy regulatory commission," 2011, http://kerea.org/wp-content/uploads/2016/08/Least-Cost-Power-Development-Plan-2011-2031.pdf.

[2] J. Lee and Z. Feng, "Gwec | global wind report 2019," 2020, https://gwec.net/wp-content/uploads/2020/08/Annual-Wind-Report_2019_digital_final_2r.pdf.

[3] M. S. Salvarli and H. Salvarli, "For sustainable development: future trends in renewable energy and enabling technologies," in *Renewable Energy-Resources, Challenges and Applications,* IntechOpen, London, UK, 2020.

[4] Ministry of Energy, "Ten Year Power Sector Expansion Energy Plan 2014-2024," 2014, https://www.coursehero.com/file/54382032/Ten-Year-Power-Sector-Expansion-Plan-2014-2024pdf/.

[5] G. M. Shafiullah, A. M. T. Oo, A. B. M. Shawkat Ali, and P. Wolfs, "Potential challenges of integrating large-scale wind energy into the power grid-A review," *Renewable and Sustainable Energy Reviews*, vol. 20, pp. 306–321, 2013.

[6] J. G. Ndirangu, J. N. Nderu, A. M. Muhia, and C. M. Maina, "Power Quality Challenges and Mitigation Measures in Grid Integration of Wind Energy Conversion Systems," in *Proceedings of the 2018 IEEE International Energy Conference (ENERGYCON)*, pp. 1–6, Limassol, Cyprus, June, 2018.

[7] S. D. Ahmed, F. S. M. Al-Ismail, M. Shafiullah, F. A. Al-Sulaiman, and I. M. El-Amin, "Grid integration challenges of wind energy: a review," *IEEE Access*, vol. 8, no. 1, Article ID 10857, 2020.

[8] C. Renewables, "Lake Turkana wind power partners with Clir renewables to optimize Africa's largest wind farm," Clir Renewable, 2021, https://clir.eco/news/lake-turkana-wind-power-partners-with-clir-renewables-to-optimize-africa-s-largest-wind-farm/.

[9] K. J. Gurubel, V. Osuna-Enciso, J. J. Cardenas, A. Coronado-Mendoza, M. A. Perez-Cisneros, and E. N. Sanchez, "Neural forecasting and optimal sizing for hybrid renewable energy systems with grid-connected storage system," *Journal of Renewable and Sustainable Energy*, vol. 8, no. 4, pp. 1–21, Article ID 045303, 2016.

[10] B. G. Brown, R. W. Katz, and A. H. Murphy, "Time series models to simulate and forecast wind speed and wind power," *Journal of Climate and Applied Meteorology*, vol. 23, no. 8, pp. 1184–1195, 1984.

[11] S. S. Soman, H. Zareipour, O. Malik, and P. Mandal, "A review of wind power and wind speed forecasting methods with different time horizons," in *Proceedings of the North American Power Symposium 2010, North American Power Symposium 2010*, pp. 1–8, Arlington, Texas, USA, October. 2010.

[12] J. Jung and R. P. Broadwater, "Current status and future advances for wind speed and power forecasting," *Renewable and Sustainable Energy Reviews*, vol. 31, pp. 762–777, 2014.

[13] W. P. Mahoney, K. Parks, G. Wiener et al., "A wind power forecasting system to optimize grid integration," *IEEE Transactions on Sustainable Energy*, vol. 3, no. 4, pp. 670–682, 2012.

[14] C. Lowery and M. O'Malley, "Impact of wind forecast error statistics upon unit commitment," *IEEE Transactions on Sustainable Energy*, vol. 3, no. 4, pp. 760–768, 2012.

[15] M. Santhosh, C. Venkaiah, and D. M. Vinod Kumar, "Current advances and approaches in wind speed and wind power forecasting for improved renewable energy integration: a review," *Engineering Reports*, vol. 2, no. 6, pp. 1–20, 2020.

[16] H. Z. Odero, C. W. Wekesa, and G. K. Irungu, "A review of wind speed and power forecasting techniques and optimal sizing of battery energy storage systems," in *Proceedings of the Sustainable Research and Innovation Conference (SRI 2021)*, pp. 19–26, Nairobi, Kenya, October 2021.

[17] K. P. Moustris, D. Zafirakis, K. A. Kavvadias, and J. K. Kaldellis, "Wind power forecasting using historical data and artificial neural networks modeling," in *Proceedings of the Mediterranean Conference on Power Generation, Transmission, Distribution and Energy Conversion (MedPower 2016)*, no. 6, p. 105, Dubrovnik, January 2016.

[18] A. Zheng and Z. Song, "Wind farm power prediction: a data-mining approach," *Wind Energy*, vol. 12, no. 3, pp. 275–293, 2009.

[19] M. Carolin Mabel and E. Fernandez, "Analysis of wind power generation and prediction using ANN: a case study," *Renewable Energy*, vol. 33, no. 5, pp. 986–992, 2008.

[20] D. A. Bechrakis and P. D. Sparis, "Correlation of wind speed between neighboring measuring stations," *IEEE Transactions on Energy Conversion*, vol. 19, no. 2, pp. 400–406, Jul 2004.

[21] M. G. De Giorgi, A. Ficarella, and M. Tarantino, "Error analysis of short term wind power prediction models," *Applied Energy*, vol. 88, no. 4, pp. 1298–1311, 2011.

[22] T. G. Barbounis, J. B. Theocharis, M. C. Alexiadis, and P. S. Dokopoulos, "Long-term wind speed and power forecasting using local recurrent neural network models," *IEEE Transactions on Energy Conversion*, vol. 21, no. 1, pp. 273–284, 2006.

[23] K. Gnana Sheela and S. N. Deepa, "An efficient hybrid neural network model in renewable energy systems," in *Proceedings of the IEEE International Conference on Advanced Communication Control and Computing Technologies (ICACCCT)*, pp. 359–361, Ramanathapuram, India, August 2012.

[24] G. Li and J. Shi, "On comparing three artificial neural networks for wind speed forecasting," *Applied Energy*, vol. 87, no. 7, pp. 2313–2320, 2010.

[25] G. Li, J. Shi, and J. Zhou, "Bayesian adaptive combination of short-term wind speed forecasts from neural network models," *Renewable Energy*, vol. 36, no. 1, pp. 352–359, 2011.

[26] E. Cadenas and W. Rivera, "Wind speed forecasting in three different regions of Mexico, using a hybrid ARIMA-ANN model," *Renewable Energy*, vol. 35, no. 12, pp. 2732–2738, 2010.

[27] J. Shi, J. Guo, and S. Zheng, "Evaluation of hybrid forecasting approaches for wind speed and power generation time series," *Renewable and Sustainable Energy Reviews*, vol. 16, no. 5, pp. 3471–3480, 2012.

[28] X. Qin, C. Jiang, and J. Wang, "Online clustering for wind speed forecasting based on combination of RBF neural network and persistence method," in *Proceedings of the 2011 Chinese Control and Decision Conference (CCDC)*, Mianyang, China, May 2011.

[29] N. Amjady, F. Keynia, and H. Zareipour, "Wind power prediction by a new forecast engine composed of modified hybrid neural network and enhanced particle swarm optimization," *IEEE Transactions on Sustainable Energy*, vol. 2, no. 3, pp. 265–276, 2011.

[30] R. Blonbou, "Very short-term wind power forecasting with neural networks and adaptive Bayesian learning," *Renewable Energy*, vol. 36, no. 3, pp. 1118–1124, 2011.

[31] Y.-Y. Hong, H.-L. Chang, and C.-S. Chiu, "Hour-ahead wind power and speed forecasting using simultaneous perturbation stochastic approximation (SPSA) algorithm and neural network with fuzzy inputs," *Energy*, vol. 35, no. 9, pp. 3870–3876, 2010.

[32] J. P. S. Catalao, H. M. I. Pousinho, and V. M. F. Mendes, "Hybrid wavelet-PSO-ANFIS approach for short-term wind power forecasting in Portugal," *IEEE Transactions on Sustainable Energy*, vol. 2, pp. 50–59, 2010.

[33] Z. Zhao Dongmei, Z. Zhu Yuchen, and Z. Zhang Xu, "Research on wind power forecasting in wind farms," *2011 IEEE Power Engineering and Automation Conference*, vol. 1, pp. 175–178, 2011.

[34] H. Liu, C. Chen, H.-q. Tian, and Y.-f. Li, "A hybrid model for wind speed prediction using empirical mode decomposition and artificial neural networks," *Renewable Energy*, vol. 48, pp. 545–556, 2012.

[35] J. P. S. Catalão, H. M. I. Pousinho, and V. M. F. Mendes, "Short-term wind power forecasting in Portugal by neural networks and wavelet transform," *Renewable Energy*, vol. 36, no. 4, pp. 1245–1251, 2011.

[36] C. Mekontso, A. Abubakar, S. Madugu, O. Ibrahim, and Y. A. Adediran, "Review of optimization techniques for sizing renewable energy systems," *Computer Engineering and Applications Journal*, vol. 8, no. 1, pp. 13–30, 2019.

[37] R. Baños, F. Manzano-Agugliaro, F. G. Montoya, C. Gil, A. Alcayde, and J. Gómez, "Optimization methods applied to renewable and sustainable energy: a review," *Renewable and Sustainable Energy Reviews*, vol. 15, no. 4, pp. 1753–1766, 2011.

[38] T. Adefarati, S. Potgieter, R. C. Bansal, R. Naidoo, R. Rizzo, and P. Sanjeevikumar, "Optimization of PV-Wind-Battery storage microgrid system utilizing a genetic algorithm," in *Proceedings of the 2019 International Conference on Clean Electrical Power (ICCEP)*, Otranto, Italy, July. 2019.

[39] Y. Liu, X. Wu, J. Du, Z. Song, and G. Wu, "Optimal sizing of a wind-energy storage system considering battery life," *Renewable Energy*, vol. 147, pp. 2470–2483, 2020.

[40] M. Sufyan, N. Abd Rahim, C. Tan, M. A. Muhammad, and S. R. Sheikh Raihan, "Optimal sizing and energy scheduling of isolated microgrid considering the battery lifetime degradation," *PLoS One*, vol. 14, no. 2, Article ID e0211642, 2019.

[41] Y. Zhang, J. Wang, A. Berizzi, and X. Cao, "Life cycle planning of battery energy storage system in off-grid wind-solar-diesel microgrid," *IET Generation, Transmission & Distribution*, vol. 12, no. 20, pp. 4451–4461, 2018.

[42] K. Hesaroor and D. Das, "Optimal sizing of energy storage system in islanded microgrid using incremental cost approach," *Journal of Energy Storage*, vol. 24, Article ID 100768, 2019.

[43] A. L. Bukar, C. W. Tan, and K. Y. Lau, "Optimal sizing of an autonomous photovoltaic/wind/battery/diesel generator microgrid using grasshopper optimization algorithm," *Solar Energy*, vol. 188, pp. 685–696, 2019.

[44] U. T. Salman, F. S. Al-Ismail, and M. Khalid, "Optimal sizing of battery energy storage for grid-connected and isolated wind-penetrated microgrid," *IEEE Access*, vol. 8, Article ID 91129, 2020.

[45] A. Navaeefard, S. M. M. Tafreshi, M. Barzegari, and A. J. Shahrood, "Optimal sizing of distributed energy resources in microgrid considering wind energy uncertainty with respect to reliability," in *Proceedings of the 2010 IEEE International Energy Conference*, Manama, Bahrain, December 2010.

[46] U. Akram, M. Khalid, and S. Shafiq, "Optimal sizing of a wind/solar/battery hybrid grid-connected microgrid system," *IET Renewable Power Generation*, vol. 12, no. 1, pp. 72–80, 2017.

[47] F. Abbas, S. Habib, D. Feng, and Z. Yan, "Optimizing Generation Capacities Incorporating Renewable Energy with Storage Systems Using Genetic Algorithms," *Electron. MDPI*, 2018.

[48] J. Dulout, B. Jammes, C. Alonso, A. Anvari-Moghaddam, A. Luna, and J. M. Guerrero, "Optimal Sizing of a Lithium Battery Energy Storage System for Grid-Connected Photovoltaic Systems," in *Proceedings of the 2017 IEEE Second International Conference on DC Microgrids (ICDCM)*, Nuremburg, Germany, June. 2017.

[49] A. Traoré, H. Elgothamy, and M. A. Zohdy, "Optimal sizing of solar/wind hybrid off-grid microgrids using an enhanced genetic algorithm," *Journal of Power and Energy Engineering*, vol. 06, no. 05, pp. 64–77, 2018.

[50] H. Fathima and K. Palanisamy, "Optimized sizing, selection, and economic analysis of battery energy storage for grid-connected wind-PV hybrid system," *Modelling and Simulation in Engineering*, vol. 2015, pp. 1–16, 2015.

[51] V. Svoboda, H. Wenzl, R. Kaiser et al., "Operating conditions of batteries in off-grid renewable energy systems," *Solar Energy*, vol. 81, no. 11, pp. 1409–1425, 2007.

[52] Meteoblue, "Weather history download Sarima," 2021, https://www.meteoblue.com/en/weather/archive/export/2.49N36.817E694_Africa%2FNairob.

[53] S. M. Gharehpetian, *Distributed Generation Systems: Design, Operation and Grid Integration*, Elsevier Science, Amsterdam, Netherlands, 2017.

[54] Asian Development Bank, *Handbook on Battery Energy Storage System*, Asian Development Bank, Mandaluyong, Philippines, 2018.

[55] H. A. Behabtu, M. Messagie, T. Coosemans et al., "A review of energy storage technologies' application potentials in renewable energy sources grid integration," *Sustainability*, vol. 12, no. 24, Article ID 10511, 2020.

[56] J. H. Holland, "Genetic algorithms," *Scientific American*, vol. 267, no. 1, pp. 66–72, 1992.

[57] X. S. Yang, *Chapter 6 - Genetic Algorithms*, Academic Press, Cambridge, MA, USA, 2021.

[58] S. Bauer, Lucas, and Matysik, "Vestas V52 - 850,00 kW - Wind-Turbine-Models.com," 2020, https://en.wind-turbine-models.com/turbines/71-vestas-v52.

[59] A. Z. Al Shaqsi, K. Sopian, and A. Al-Hinai, "Review of energy storage services, applications, limitations, and benefits," *Energy Reports*, vol. 6, pp. 288–306, 2020.

[60] Lake Turkana Wind Power, "Sustainability Performance Report: Powering the Nation," 2019, https://ltwp.co.ke/newsite/wp-content/uploads/LTWP-2019-Sustainability-Performance-Report-v4.pdf.

[61] C. Oludhe, "Assessment and utilization of wind power in Kenya-a review," *J Kenya Meteorol Soc*, vol. 2, pp. 39–52, 2008.

[62] T. Ma, H. Yang, and L. Lu, "A feasibility study of a stand-alone hybrid solar-wind-battery system for a remote island," *Applied Energy*, vol. 121, pp. 149–158, 2014.

[63] L. Lin Xu, X. Xinbo Ruan, C. Chengxiong Mao, B. Buhan Zhang, and Y. Yi Luo, "An improved optimal sizing method for wind-solar-battery hybrid power system," *IEEE Transactions on Sustainable Energy*, vol. 4, no. 3, pp. 774–785, 2013.

[64] S. Teleke, M. E. Baran, S. Bhattacharya, and A. Q. Huang, "Rule-based control of battery energy storage for dispatching intermittent renewable sources," *IEEE Transactions on Sustainable Energy*, vol. 1, no. 3, pp. 117–124, 2010.

[65] T. K. A. Brekken, A. Yokochi, A. von Jouanne, Z. Z. Yen, H. M. Hapke, and D. A. Halamay, "Optimal energy storage sizing and control for wind power applications," *IEEE Transactions on Sustainable Energy*, vol. 2, no. 1, pp. 69–77, 2010.

[66] Q. Li, S. S. Choi, Y. Yuan, and D. L. Yao, "On the determination of battery energy storage capacity and short-term power dispatch of a wind farm," *IEEE Transactions on Sustainable Energy*, vol. 2, no. 2, pp. 148–158, 2011.